REPORT

Reinforcement measures IJsselbrug A12

Bridge

Customer: Rijkswaterstaat

Reference: T & P-BF7387-R007-F2.0

Status: 2.0 / Final

Date: March 10, 2020

Project related

HASKONINGDHV NEDERLAND BV

Box 151
6500 AD Nijmegen
Transport & Planning
Trade register number: 56515154

+31 88 348 70 00 T
+31 24 323 93 46 F
info@rhdhv.com E
royalhaskoningdhv.com W.

Title document: Reinforcement measures IJssel bridge A12

Subtitle:
Reference: T & P-BF7387-R007-F2.0
Status: 2.0 / Final
Date: March 10, 2020
Project name: Recalculation and reinforcement design IJsselbrug A12
Project number: BF7387
Author (s): A. Akyel, E. Klamer

Prepared by: A. Akyel, E. Klamer

Checked by: R. Soetekouw

Date / initials: 3/10/2020

Approved by: K. Vis

Date / initials: 3/10/2020

Classification

Project related

Project related

Content

Attachments

Version	Adjustment	Date
D0.1	First draft version, internal review	3/20/2019
D0.2	Second draft version, to test Rijkswaterstaat	4/12/2019
D0.3	Remarks Rijkswaterstaat processed, internal review	5/17/2019
F1.0	First final version	5/28/2019

F1.1	Burr grinding at the welding gates removed (section 4.13) Fatigue calculation at interrupted fillet weld longitudinal direction enclosure added (section 4.5.1) Fatigue calculation at x-seam body and connection body main beam - transverse stiffeners adjusted (sections 4.5.2 and 4.10) Welding end of T-piece adjusted to 1000 mm	7/24/2019
F2.0	- Reinforcements of cross beams added (sections 4.9 to 4.11, chapter 7) - References TNO and IIW added (section 1.1)	10/2020

Project related

1 Reading Guide

This report describes the reinforcement measures for the bridge (s) of the IJsselbrug A12 including its structural design calculations. This report must be submitted be read in conjunction with the following reports

- Basic report recalculation IJssel bridge A12 [T & P-BF7387-R001],
- Verification calculations IJsselbrug A12 Bridgeing [T & P-BF7387-R005]
- Technical requirements for reinforcement measures Bridge IJssel bridge A12 [T & P-BF7387-R011]

Bridge Bridge Main bridge

Figure 1 Side view of the IJssel bridge [A.46205A]

From the verification calculation [T & P-BF7387-R005] it follows that only the cross stiffeners and the jacking points of the portals at the end supports are not strong enough. The rest of the construction is satisfactory principle on strength in the current situation. On fatigue both the various details in the main beam if the details in the cross beam connections are not. Therefore, there is for the calculations chosen to first calculate the reinforcements for fatigue, and only then to discuss the strength of the construction. The content of this report is therefore in a different order from the verification calculations.

In order to improve the different fatigue details in the main beam, we are initially looking at it whether “simple” measures (burr grinding, coring out rivets) can reduce the current fatigue damage can be removed and the detail class can be increased, so that damage will be below D = by the end of 2050 1.0 comes. The results of this analysis are discussed in Chapter 2.

This analysis shows that this is not sufficient without the additional amplification achieve a fatigue life of 30 years. Therefore, chapter 3 describes the amplification at reduce the tensions and address the adjustments needed to the modeling.

In chapter 4, the results of the fatigue analysis for the reinforced situation. Chapter 5 will then check whether the strengths stability tests of the main supporting structure still comply with the reinforcements. Hereby will the reinforcement of the vertical is also discussed. Chapter 6 describes the connections and the results are summarized in chapter 7.

Project related

1.1 References

In addition to the references in the basic report, the following reports have been used for the reinforcement design:

[1] TNO Report TNO-2017-R11499. Various fatigue advice for the bridge near Rheden, 2017
[2] TNO Note 100315818 / ALL. Fatigue classification of fillet welds in crotch and T-joints. 2018
[3] TNO Report TNO-2018-R11423. Fatigue IJssel bridge Rheden - not absorbing force rivets, 2018
[4] TNO Report TNO-2018-R10290B. Description of preventive emergency repairs for the bridge at Rheden, 2018
[5] TNO Report TNO-2019-R11393. Rack measurements IJsselbrug, 2019
[6] TNO Report TNO-2019-R11394. Various advice on fatigue life crossbeam connections IJsselbrug, 2020
[7] TNO Report TNO-2019-R10527. Risk analysis of welding imperfections in the IJsselbrug A12, 2019
[8] TNO Report TNO-2020-R10226. Rack measurements IJsselbrug - Additional measurements December 2019, 2020
[9] IIW Document IIW-2259-15 ex XIII-2460-13 / XV-1440-13. Recommendations for Fatigue Design of Welded Joints and Components, 2016
[10] IIW-Doc. XIII-2380r3-11 / XV-1383r3-11. IIW Guideline for the Assessment of Weld Root Fatigue, 2012

2 Testing for fatigue after improving connections

The verification calculations showed that most connections in the bridges do not meet the fatigue requirement of D ≤ 1.0 at γ_{Mf} = 1.35 at the end of 2050. Starting point in this The calculation is that the parts that do not meet this requirement need to be reinforced. This chapter is looked at the feasibility of using relatively simple improvement techniques (burr grinding, drill out rivet holes) it is possible to remove the existing fatigue damage and remove the detail category, in order to still meet the fatigue requirement. For the calculations in this The chapter therefore still assumes the current unamplified situation.

The calculations in this report have been calculated for all main beams, including as part of the beams do not need to be strengthened. Therefore, the following color coding is used for the results after a certain proposed reinforcement.

1.0	Needs reinforcement, satisfactory after proposed reinforcement
1.2	Needs to be amplified, but not satisfactory after suggested amplification
0.0	Does not need to be amplified, suffices if the proposed amplification is nevertheless carried out
1.2	Does not need to be reinforced, is not sufficient if the proposed reinforcement is nevertheless carried out

Table 1 Color coding results after amplification

2.1 Type 1: Weld end on bottom plate flange of main beam

The fillet welds on the ends of the filler plates in the bridges are not fatiguing. Figure 2 provides an overview of the locations where this connection is located.

Figure 2 Location of the connection type 1.

The table below gives the results of the damage calculations, if nothing is done about the connections would be done. The explanation of this calculation is given in the report of the verification calculation [T & P-BF7387-R005]

γ_{Mf} = 1.35	**HRB west**		**HRB east**		**PRB west**		**PRB east**	
Year	**2018**	**2050**	**2018**	**2050**	**2018**	**2050**	**2018**	**2050**
1-1 / 1-8	3.3	10.5	1.7	2.2	3.3	6.9	0.2	0.5
1-2 / 1-7	8.9	28.3	5.8	7.8	8.8	18.5	0.9	1.9
1-3 / 1-6	1.1	4.0	0.6	0.8	1.1	2.5	0.1	0.2
1-4 / 1-5	1.3	4.5	0.7	0.9	1.3	2.9	0.1	0.2

Table 2 Damage figures for connection type 1 for the end of 2018 and the end of 2050.

Because various welding and adhesion errors have been found, it is recommended that all joints are used recover, even those that would do arithmetically by the end of 2050.

It is noted that the preventive is not taken into account in the table above
reinforcements that will be in 2018 and implemented in 2019. This concerns the following locations

- HRB west 1-2 and 1-7 (both bridges) (2018)
- PRB west 1-2 and 1-7 (both bridges) (2018)
- HRB eastern 1-7 (2 E aanbrug) (2019)
- PRB western 1-1 (1 e aanbrug) (2019)
- PRB west 1-8 (1 e aanbrug) (2019)
- PRB west 1-8 (2 E aanbrug) (2019)

Initially, it was examined whether the various connections to the preventive measures designed by TNO strengthening of connections 1-2 in HRB west and PRB west, see report TNO-2018-R10290B [4] , can be permanently restored. With this repair measure, the weld is placed on the end of the thickening plate removed (including root of the weld) and replaced with a new weld, which is expanded under an angle of 20 ° to 30 °, see Figure 3 . The new weld should gradually transfer at 100 mm from the corner go into the existing fillet weld. Grinding the old weld and burr grinding the bottom flange any fatigue damage present at the original toe of the weld to be removed. After re-welding, the new welding stone must be cut with a milling burr (burr grinding) be machined to improve the fatigue strength of the weld. According to IIW report Recommendations for Fatigue Design of Welded Joints and Components [9] takes the fatigue strength of the weld joint 30% after burr grinding the welding stone. The detail category of the improved, new weld can therefore be held at $\Delta\sigma_c = 58 * 1.3 = 75.4$. (NB the detail category of this connection (without burr grinding) has been determined by TNO with the help of a hot-spot stress approach DC = 58 (TNO-2017-R11499 [1]) .

Figure 3 Reinforcement of the welds on the ends of the thickening plates.

The damage numbers have been recalculated for the connections, assuming the current ones damage can be zeroed and based on the improved detail category of 75.4. The results for the different main beams for $\gamma_{Mf} = 1.35$ are shown in Table 3 .

$\gamma_{Mf} = 1.35$	HRB west	HRB east	PRB west	PRB east
Year	2050	2050	2050	2050
1-1	3.0	0.2	1.5	0.1
1-2	10.2	0.9	5.1	0.4
1-3	1.0	0.1	0.5	0.0
1-4	1.4	0.1	0.7	0.0

Table 3 Damage figures of the connection type 1 burr grinding of the weld before the end of 2050.

The connections in the main carriageway west and part of the connections in the parallel carriageway west appear despite this improvement, it does not meet the damage requirement $D \leq 1.0$ at $\gamma_{Mf} = 1.35$.

It is concluded that in addition to improving the weld, additional measures are also necessary to make the connection work. In section 4 .1 will therefore be given to the design of the reinforcement to reduce the stresses in the joints.

It is noted that account is taken in particular for connection 1-2 of the HRB west and PRB west it should be that the amplification has already been performed. Approximately D = 0.3 arrives in HRB West every year damage, as long as there is not yet reinforced. This is half for the PRB West (D = 0.15 per year).

2.2 Type 2: Riveted joints in section sections of the bridge

The fatigue calculations of the existing situation show that the riveted joints in the lower flange (and part of the web) of the main beam does not meet the damage requirement $D \leq 1.0$ at $\gamma_{Mf} = 1.35$ at the end of 2050.

2-1 2-2 2-3 2-4

Figure 4 The locations of the riveted joints in the type 2 main beam.

$\gamma_{Mf} = 1.35$	HRB west		HRB east		PRB west		PRB east	
Year	**2018**	**2050**	**2018**	**2050**	**2018**	**2050**	**2018**	**2050**
2-1	0.3	1.4	0.1	0.2	0.3	0.8	0.0	0.0
2-2	0.5	1.8	0.2	0.3	0.5	1.1	0.0	0.1
2-3	0.5	1.7	0.3	0.4	0.4	1.1	0.0	0.1
2-4	0.4	1.6	0.2	0.2	0.4	1.0	0.0	0.0

Table 4 Damage figures for connection type 2 (bottom flange) for the end of 2018 and the end of 2050.

Consider using rivets to strengthen the joints that are not satisfactory
replaced by preload injection bolts, by drilling them out one by one, drilling the holes slightly (1 a
2 mm), so that the fatigue damage is removed (check by NDT) and one
replace the preload injection bolt at the front.

NEN-EN 1993-1-9 indicates that connections with prestressed injection bolts with
detail category 112 may be calculated on the basis of the stresses in the gross section, see
Figure 5.

Figure 5 Detail category for the connections with prestressed injection bolts, according to EN 1993-1-9.

Normally, a pretension injection bolt connection can both butt (through the resin) and friction (through the
preload). For the connection in the IJsselbrug, however, it is plausible that there is
Menie is used between the plates, so it is not possible to assume frictional resistance. In
In consultation with TNO, it has therefore been determined that for such a connection, the
detail category of fitting bolts, with detail category 90. This should be based on the
tensions in the net cross-section.

Figure 6 Detail category for the connections with fitting bolts, according to EN 1993-1-9.

The damage numbers have been recalculated for the connections, assuming the current ones
damage can be set to zero by drilling the hole and assuming a detail category 90.
The test results for the different main beams for γ_{Mf} = 1.35 are shown inTable 5. The
cells with a white background do not need to be amplified in principle, but are for the
completeness calculated.

γ_{Mf} = 1.35	HRB west	HRB east	PRB west	PRB east
Year	**2050**	**2050**	**2050**	**2050**
2-1	1.0	0.0	0.5	0.0
2-2	1.2	0.1	0.6	0.0
2-3	1.2	0.1	0.6	0.0
2-4	1.1	0.1	0.6	0.0

Table 5 Damage figures for the type 2 connection after replacing rivets for pretension injection bolts before the end of 2050.

The connections in the western main girder of the main carriageway just fail to meet the
damage claim D ≤ 1.0 at γ_{Mf} = 1.35. Because the current damage is currently at most D = 0.5, and before it
type 1 already requires a reinforcement to realize a voltage reduction in the lower flange
it makes more sense to apply the reinforcement with the tee also here and to ensure that the already
damage present plus the damage will not increase between now and the end of 2050 if D = 1.0. It is not then

needed to replace the rivets. This will be further elaborated in section 4.2.

2.3 Type 3 Vertical pleat stiffeners inside - weld with bottom flange of the main beam

The body of the main beams is stiffened with a half DIN 32 profile in the transverse direction of the body (transverse stiffener). The flange of the stiffener is chamfered at the bottom and together with a part of the stiffener body welded to the bottom flange. This weld joint has been tested on the basis of the voltage change in the bottom flange of the main beam. The calculation shows that most compounds do not meet the damage requirement D ≤ 1.0 at $\gamma_{Mf} = 1.35$, with the exception of the eastern one beam of the parallel carriageway.

Figure 7 The locations of the type 3 connections.

$\gamma_{Mf} = 1.35$	HRB west		HRB east		PRB west		PRB east	
Year	**2018**	**2050**	**2018**	**2050**	**2018**	**2050**	**2018**	**2050**
3-1	0.5	1.7	0.3	0.4	0.4	1.1	0.0	0.0
3-2	0.9	3.3	0.5	0.6	0.9	2.1	0.0	0.1
3-3	1.9	6.5	1.0	1.2	1.8	4.1	0.1	0.2
3-4	1.9	6.4	1.0	1.3	1.8	4.1	0.1	0.2
3-5	1.4	4.7	0.7	0.9	1.4	3.0	0.1	0.2
3-6	1.9	6.4	1.0	1.3	1.9	4.2	0.1	0.3
3-7	0.2	0.6	0.1	0.1	0.2	0.4	0.0	0.0
3-8	0.1	0.5	0.0	0.1	0.1	0.3	0.0	0.0
3-9	0.2	0.8	0.1	0.2	0.2	0.5	0.0	0.0
3-10	1.5	5.1	1.0	1.3	1.5	3.3	0.1	0.2
3-11	2.6	8.7	1.6	2.1	2.6	5.6	0.2	0.4
3-12	2.5	8.6	1.5	1.9	2.5	5.5	0.2	0.4

Table 6 Damage figures for connection type 3 for the end of 2018 and the end of 2050.

To improve the detail category of the weld and remove the damage, if reinforcement measure initially considered burr grinding of the weld joint. The critical one location for the initiation of fatigue cracks is in the weld joint of the fillet weld. By means of burr grinding grind the weld stone to remove the current fatigue damage and a

Page 15

Figure 8). According to IIW report "Recommendations for Fatigue Design of Welded Joints and Components"
[9] this process provides a 30% improvement in the detail category. After burr grinding can therefore be counted with a detail category of $\Delta\sigma_c = 80 * 1.3 = 104$ and damage can be assumed
D = 0.0 just after burr grinding.

Figure 8 Location of the burr to be welded with the bottom flange of the main beam (shown in red)

The improved situation was calculated every 5 meters for two different ones
safety factors γ_{Mf} = 1.35 and 1.15. A dynamic magnification factor has been taken into account
the joint transitions of $\Delta\varphi_{fat}$ = 1.15, where applicable. The test results are for the
different main beams for γ_{Mf} = 1.35 are shown in Table 7. The cells with white background
in principle do not have to be burr-gravel, because they are sufficient. For completeness, the
results displayed. In particular in the main carriageway west and to a lesser extent in the parallel carriageway
West shows that the damage requirement D ≤ 1.0 cannot yet be met if γ_{Mf} = 1.35.

γ_{Mf} = 1.35	HRB west	HRB east	PRB west	PRB east
Year	2050	2050	2050	2050
3-1	0.3	0.0	0.2	0.0
3-2	0.8	0.0	0.4	0.0
3-3	1.8	0.1	0.9	0.0
3-4	1.7	0.1	0.9	0.0
3-5	1.2	0.1	0.6	0.0
3-6	1.7	0.1	0.9	0.1
3-7	0.1	0.0	0.1	0.0
3-8	0.1	0.0	0.0	0.0
3-9	0.2	0.0	0.1	0.0
3-10	1.3	0.1	0.6	0.0
3-11	2.4	0.2	1.2	0.1
3-12	2.3	0.2	1.2	0.1

Table 7 Damage figures of the Type 3 connection after burr grinding on the welding stone before the end of 2050.

In order to nevertheless meet the damage requirement D ≤ 1.0, it will also be necessary for this type of connection
decrease the tension in the bottom flange. Alternatively, the weld could be removed and removed
to be replaced for a bolted connection. Considering the number of reinforcements needed and the fact that there is anyway
if voltage reduction is necessary for the type 1 and type 2 connections, it makes more sense to use the
decrease voltage. This reinforcement will be further elaborated in section 4.3.

2.4 Type 4: Riveted crossbeam connection to the main beams

From the fatigue calculations of the riveted connection of the cross braces to the bottom flange of the main beam, it appears that a limited number of connections is not sufficient.

Figure 9 The locations of the riveted joints in the type 4 main beam.

γ_{Mf} = 1.35	HRB west		HRB east		PRB west		PRB east	
Year	**2018**	**2050**	**2018**	**2050**	**2018**	**2050**	**2018**	**2050**
4-1	0.1	0.4	0.0	0.0	0.1	0.2	0.0	0.0
4-2	0.3	1.3	0.1	0.1	0.2	0.8	0.0	0.0
4-3	0.3	1.2	0.1	0.1	0.3	0.7	0.0	0.0
4-4	0.0	0.0	0.0	0.0	0.0	0.0	0.0	0.0
4-5	0.2	0.8	0.1	0.1	0.2	0.5	0.0	0.0
4-6	0.5	2.1	0.2	0.3	0.4	1.2	0.0	0.0

Table 8 Damage figures for connection type 4 for the end of 2018 and the end of 2050.

To improve the detail category, consider removing the rivets, the
remove damage by clearing the holes and replacing the preload injection bolts. Because there
probably menie is applied between the contact surfaces can not be guaranteed that one
good friction surface is created between the plates. The detail category is therefore maintained at DC = 90,
although there is no force-bearing connection. It is noted that this is lower than the
originally held category for the rivet joint ($\Delta\sigma_c$ = 101). The
calculation results are shown in Table 11 . Basically, the cells with a white background are required
not to be strengthened, but are calculated for completeness.

γ_{Mf} = 1.35	HRB west	HRB east	PRB west	PRB east
Year	**2050**	**2050**	**2050**	**2050**
4-1	1.5	0.1	0.7	0.0
4-2	3.0	0.2	1.5	0.1
4-3	3.0	0.2	1.5	0.1
4-4	0.1	0.0	0.1	0.0
4-5	2.3	0.2	1.2	0.1
4-6	4.0	0.3	2.0	0.1

Table 9 Damage figures for the Type 4 connection after replacing rivets for pretension injection bolts before the end of 2050.

The test results indicate that replacing the rivets with pretension injection bolts does not
makes sense, if it is assumed that $\Delta\sigma_c$ = 90. Because there should already be voltage reduction
it makes more sense to leave the rivets in place and reduce the tension so that the
damage remains below D = 1.0 by the end of 2050. This is further elaborated in section 4.4.

2.5 Type 5: Welded connection in the section sections of the bridge

2.5.1 V-weld bottom flange

In a number of locations, the plates are interconnected in the bottom flange by means of a V-weld. from
The fatigue analysis of the existing situation showed the following results.

Figure 10 The locations of the welded joint in the type 5 main beam.

γ_{Mf} = 1.35	HRB west		HRB east		PRB west		PRB east	
Year	**2018**	**2050**	**2018**	**2050**	**2018**	**2050**	**2018**	**2050**
5-1	1.7	5.9	1.0	1.2	1.7	3.8	0.1	0.2
5-2	2.7	9.1	1.5	1.9	2.7	5.9	0.2	0.4
5-3	4.1	13.3	2.5	3.4	4.0	8.6	0.3	0.7

Table 10 Damage figures for connection type 5 (bottom flange) for the end of 2018 and the end of 2050.

Burr grinding can be used as a possible improvement technique. Because in the first and
In the third field when a screed plate is used, it is not possible to burr both sides of the weld.
For the flat-ground side, a higher detail category ($\Delta\sigma_c$ = 112) than the current can be used for the welding stone
held $\Delta\sigma_c$ = 71 are held, because it has been ground flat in the past, but for the
on the plate with the welding root on top, this is not possible. Therefore, $\Delta\sigma_c$ must be assumed for this
= 71 (detail 14 in accordance with table 8.3 of NEN-EN 1993-1-9). For details 5-1 and 5-2 it has burr grinding
so no use and the connection has to be over-bridged. This is further elaborated in section 4.5 .

$\Delta\sigma_c$ = 71

$\Delta\sigma_c$ = 112

$\Delta\sigma_c$ = 71

$\Delta\sigma_c$ = 71

Figure 11 V-weld in the bottom flange and top plate of the main beam and the detail category for the root and toe of the welds.

For compound 5-3 it is possible to use gravel on the top and bottom. This can cause damage
be brought back to D = 0.0.

Figure 12 Burr grinding of the weld type 5-3

It is believed that burr grinding can increase the detail category by 30% [9] . After
burr grinding can therefore be calculated with a detail category of $\Delta\sigma_c$ = 71 * 1.3 = 92.3. For the
part under the body, which is not accessible, according to TNO it can be assumed that fatigue is not
will be decisive, because the growth of any defect will be prevented by the longitudinal weld
between body and flange. This will prevent the crack from opening. The results of the
fatigue calculation of this compound is shown for γ_{Mf} = 1.35 inTable 11.

γ_{Mf} = 1.35	HRB west	HRB east	PRB west	PRB east
Year	**2050**	**2050**	**2050**	**2050**

5-3	3.8	0.3	1.9	0.1

Table 11 Damage figures for the Type 5-3 compound in field 2 after burr grinding before the end of 2050.

The results show that despite the welding improvement, the fatigue strength at the end of 2050 is not sufficient for the western main beams without reinforcement. Here, too, it will therefore be necessary to reduce the tensions reduce. Since the damage is currently at or above 1.0, this must be combined with burr grinding of the weld (with the exception of the parallel runway east). The reinforcement necessary is to reduce the voltage will be tested in section 4.5 .

2.5.2 X-welded body

The x-weld in the body does not meet the bottom of the body in the current situation either.

$\gamma_{Mf} = 1.35$	HRB west		HRB east		PRB west		PRB east	
Year	**2018**	**2050**	**2018**	**2050**	**2018**	**2050**	**2018**	**2050**
5-1	0.6	2.1	0.3	0.4	0.5	1.3	0.0	0.1
5-2	1.0	3.4	0.5	0.6	1.0	2.2	0.0	0.1
5-3	1.6	5.4	1.0	1.3	1.6	3.5	0.1	0.2

Table 12 Damage figures for connection type 5 (bottom of body) for the end of 2018 and the end of 2050.

Burr grinding can also be used here. Because the connection still needs to be strengthened and the voltage will be reduced as a result, section 4.5 will first consider which part of the body in the fortified situation still needs burr grinding. Given the current damage, it is likely that this is not necessary for connection 5-1 and for the PRB east.

2.6 Type 6: Flank seal between the cover plate and the bottom flange

For the flank weld between the top plate and the bottom flange, only one in the western main beams becomes one exceeding the fatigue damage found in the first span.

Figure 13 Tested locations of the connection type 6.

$\gamma_{Mf} = 1.35$	HRB west		HRB east		PRB west		PRB east	
Year	**2018**	**2050**	**2018**	**2050**	**2018**	**2050**	**2018**	**2050**
6-1	0.3	1.2	0.2	0.2	0.3	0.7	0.0	0.0
6-2	0.8	2.8	0.3	0.4	0.7	1.7	0.0	0.1
6-3	0.8	2.7	0.4	0.5	0.7	1.7	0.0	0.1
6-4	0.5	1.9	0.2	0.3	0.5	1.2	0.0	0.1
6-5	0.0	0.1	0.0	0.0	0.0	0.1	0.0	0.0

Table 13 Damage figures for connection type 6 before the end of 2018 and the end of 2050.

Burr grinding the flank weld will not so much increase the detail category, but it can the current damage can be removed. This is because burr grinding is for improvement of the welding toe, the voltage occurring perpendicular to the welding toe and not, as in this case, parallel on the weld. Given the dimensions of the current weld (a = 4 mm), the weld should be used again after burr grinding to be expanded. The connection has therefore been considered based on the detail category $\Delta\sigma_c$ = 100, with damage starting at zero in 2018. Weld at the location of the white cells in the table below in principle do not need to be improved, but have been calculated for completeness.

$\gamma_{Mf} = 1.35$	HRB west	HRB east	PRB west	PRB east
Year	**2050**	**2050**	**2050**	**2050**
6-1	0.9	0.0	0.5	0.0
6-2	2.0	0.1	1.0	0.0

6-3	2.0	0.1	1.0	0.1
6-4	1.4	0.1	0.7	0.0
6-5	0.1	0.0	0.0	0.0

Table 14 Damage figures for the Type 6 connection after burr grinding before the end of 2050.

In particular for HRB West, only applying burr grinding is therefore insufficient. Here too will the tension lowered by increasing the bottom flange. For this reference is made to paragraph 4.6.

2.7 Type 13: Flank weld between the web and the bottom flange of the main beam

For compound type 13, the following damage numbers have been found in the recalculation. Here is every 5 m tested, with the locations corresponding to type 3.

$\gamma_{Mf} = 1.35$	HRB west		HRB east		PRB west		PRB east	
Year	**2018**	**2050**	**2018**	**2050**	**2018**	**2050**	**2018**	**2050**
13-1	0.1	0.5	0.1	0.1	0.1	0.3	0.0	0.0
13-2	0.3	1.2	0.2	0.2	0.3	0.8	0.0	0.0
13-3	0.8	2.8	0.3	0.4	0.7	1.7	0.0	0.1
13-4	0.8	2.7	0.4	0.5	0.7	1.7	0.0	0.1
13-5	0.5	1.9	0.2	0.3	0.5	1.2	0.0	0.1
13-6	0.8	2.7	0.4	0.5	0.8	1.7	0.0	0.1
13-7	0.0	0.2	0.0	0.0	0.0	0.1	0.0	0.0
13-8	0.0	0.1	0.0	0.0	0.0	0.1	0.0	0.0
13-9	0.1	0.2	0.0	0.0	0.0	0.1	0.0	0.0
13-10	0.6	2.1	0.4	0.5	0.5	1.3	0.0	0.1
13-11	1.1	3.8	0.7	0.9	1.1	2.4	0.1	0.2
13-12	1.1	3.7	0.6	0.8	1.0	2.4	0.1	0.1

Table 15 Damage figures for connection type 13 for the end of 2018 and the end of 2050.

The same applies for this connection as for type 6, only the damage due to burr grinding can be taken away. The detail category will in principle not improve. Because for the earlier If a voltage drop is necessary after all, this connection is no longer calculated without amplification. For the calculation of the reinforced situation, see section 4.8.

2.8 Type 17: Vertical pleat stiffeners - weld with main beam web

The body of the main beams is with each cross beam with a half INP 32 profile in the transverse direction of the body stiffened (stiffener). At the supports, two ½ INP 32 profiles are used on either side of the body. The body of the pleat stiffener is welded to the body with a fillet weld a = 4 mm. The assessments of these connections are made every 5 m. The calculation of the current situation has shown that the most compounds do not meet the damage requirement D ≤ 1.0 at γ_{Mf} = 1.35, with the exception of the eastern beam of the parallel carriageway.

17-12 17-11 17-10 17-9 17-8 17-7 17-6 17-5 17-4 17-3 17-2 17-1

Figure 14 The locations of the type 17 connections.

γ_{Mf} = 1.35	HRB west		HRB east		PRB west		PRB east	
Year	2018	2050	2018	2050	2018	2050	2018	2050
17-1	0.4	1.4	0.3	0.3	0.4	0.9	0.0	0.0
17-2	0.7	2.7	0.4	0.5	0.7	1.7	0.0	0.1
17-3	1.5	5.4	0.8	1.0	1.5	3.4	0.1	0.2
17-4	1.5	5.3	0.8	1.0	1.5	3.4	0.1	0.2
17-5	1.1	3.8	0.5	0.7	1.1	2.5	0.0	0.1
17-6	1.7	5.6	0.8	1.1	1.7	3.6	0.1	0.2
17-7	0.1	0.5	0.0	0.1	0.1	0.3	0.0	0.0
17-8	0.1	0.4	0.0	0.0	0.1	0.2	0.0	0.0
17-9	0.2	0.6	0.1	0.1	0.1	0.4	0.0	0.0
17-10	1.3	4.4	0.8	1.1	1.3	2.8	0.1	0.2
17-11	2.2	7.5	1.4	1.8	2.2	4.8	0.2	0.4
17-12	2.2	7.4	1.2	1.6	2.2	4.8	0.1	0.3

Table 16 Damage figures for connection type 17 for the end of 2018 and the end of 2050.

To improve the detail category of the weld and to remove the damage, you can also do this here reinforcement measure burr grinding of the weld joint. From the calculations of type 3 has already been shown that this will not be sufficient and that voltage reduction will be necessary. In paragraph 4.12 will therefore examine whether this is possible after the voltage drop in the main beam.

3 Reinforcements

3.1 Reinforcement main beam

The calculations in the previous section have shown that it is necessary to reduce the stresses. For this purpose, a T-piece is fitted under the main beam over almost the entire length of the fields. This is not necessary only at the location of the supports.

Figure 15 Bridge side view with reinforcement of the bottom flange shown in red.

The tee is composed of a body of 15x350 mm and a flange of 500x35 mm, which is under the existing bottom flange are welded.

Figure 16 Principle section across the lower flange with reinforcement (stiffeners and cross stiffeners not shown).

At the end of the T-piece, the flange is tapered and there is a rounding in the body of the Tbroken towards the existing bottom flange, to obtain a gradual voltage transfer from the tee to the existing bottom flange.

Figure 17 Principle cross-section termination T-piece

To prevent the bridge from becoming asymmetrical, the reinforcement on both the western and the eastern main beam applied.

3.2 Other reinforcements

In addition to the aforementioned reinforcement of the main beam for fatigue, there are a number of additional locally reinforcements necessary, in addition to improving various welds. This concerns the following reinforcements:

- Casing v-seams lower flange (fatigue) (sections 4.5 and 6.7)
- Bottom vertical portal end supports (strength) (section 5.3.2)
- Jacking points end supports (strength) (section 5.6.2)
- Connection lower edge of fixed supports (connection) (section 6.3)

These reinforcements are detailed in the aforementioned sections. Because these are local reinforcements, they do not affect the modeling.

3.3 Modeling adjustment

For the modeling, the T-piece under the main beam has been added to the finite element model has also been used for the verification calculations of the current situation. For this, use was made of an extra construction phase in which the T-piece is added to the cross-section. This is in the first 10 construction phases the T-piece is not yet available, from phase 11 it will be added to the cross-section. Because of this, the permanent load is only carried by the old profile, but it becomes additional weight of the tee and variable loads, however, due to the reinforced profiles behave.

Phase Model	Change of construction	Tax case

Phase 1 Global model	Add steel construction with tpv main beam intermediate support only lower flange and web	Own weight of steel
Phase 2 Global model -		Bulk density prestressed concrete deck
Phase 3 Model concrete deck	Separate model with prestressed concrete deck (eg = 0) + top flange main beam (T)	Preload
Phase 4 Global model	Add top flange main beam at intermediate support + prestressed concrete deck	Jacking
Phase 5 Global model -		Bulk density reinforced concrete deck
Phase 6 Global model Add reinforced concrete deck (eg = 0)		Indulgences
Phase 7 Global model -		Asphalt pavement
Phase 8 Global model -		Other permanent taxes
Phase 9 Global model -		Shrink and creep
Phase 10 Global model -		Prestressing loss
Phase 11 Global model Add tee		T-piece own weight
Phase 12 Global model -		Variable taxes

Table 17 Overview of modeled construction phases

Figure 18 T-piece under the main girder in construction phase 11

Project related

Figure 19 Detail of intermediate support point with the T-piece under the bottom flange in green

A local plate model has been drawn up for the termination of the tee, see section 6.6 .

3.4 Adjustment of taxes

Basically, the same taxes were used as for the verification calculations. There are, however, a number made minor changes. For example, a load case has been added with the weight of the T-piece. The own weight is determined automatically by SCIA.

In addition, the wind load has been adjusted, because the beams have become slightly higher and therefore more catch wind. For this, the point load at the bottom of the K-bandages has been increased by 0.385 m * 10 m * q_{wind} for the k-bandages and half for the end supports.

The other taxes remained the same.

4 Fatigue test after reinforcement

This chapter will demonstrate per type that the (normative) connection meets the fatigue requirement D ≤ 1.0 at $\gamma_{Mf} = 1.35$. In the SCIA calculation the cross-sections of the The main beam and the cross stiffeners at the portals have been adjusted and are the influence lines of the connections redefined, based on the new stiffness ratios. With these new lines of influence, the fatigue calculation of the connections performed again. Besides the existing connections are the new connections were also tested. These start at type 20.

In addition, reference is made to the report “TNO-2019-R10527 Risk analysis of welding imperfections in the IJssel bridge A12 ” [7] . It has been shown that, with the exception of some v-welds in the bottom flange (type 5), no welding impacts were found with a residual life of less than 30 years. In addition, a probabilistic analysis has also determined this based on the defects found the risk from non-inspected locations is acceptable.

4.1 Type 1: Weld end on bottom plate flange of main beam

Given that the current damages for most type 1 connections are currently above 1.0 and adhesion errors in the weld have been found during inspections, will be taken as final repair measure proposed to reinforce all welds in addition to reinforcing the bottom flange with the T-profile to be replaced at the location of the ends of the thickening plates and to be removed in accordance with the method as has been used as a preventive reinforcement for the connection of type 1-2 HRB west and PRB west, see report [R10290B]. This includes grinding away the weld, including grinding away the current damage, and re-welding and removing the weld at an angle of 20 ° to 30 °, shown in red in the figure below. Then the toe of the new weld burr grinding should be applied, to increase fatigue strength. For the full description of the steps to be performed, see refer to report T & P-BF7387-R011.

Figure 20 Reinforcement of the welds on the ends of the thickening plates

From a practical point of view (inspection, execution) and fatigue technical point of view, local, on site at the end of the thickening plate, a recess in the body of the T-piece must be made, so that there no (extra) voltage peaks occur at the welding ends of the screed plate. Becomes assumes an opening of 50 mm. This is taken into account in the determination of the tensions by not including this part of the body in the cross-sectional properties. Fatigue from the detail of the weld at the end of the opening will be treated in type 20.

Figure 21 Side view of the recess at the end of the thickening plate

For the fatigue detail of the weld at the end of the thickening plate, the fatigue analysis has been repeated executed. The starting point is that there is no more damage after burr grinding and therefore D = 0 is allowed are going out. The damage development between now and (late) 2050 has subsequently been calculated with a (improved) detail category of $\Delta\sigma_c$ = 58 * 1.3 = 75.4. The test results are shown in Table 18 .

γ_{Mf} = 1.35	HRB west	HRB east	PRB west	PRB east
	2050	2050	2050	2050
1-1 / 1-8	0.0	0.0	0.0	0.0
1-2 / 1-7	0.3	0.0	0.1	0.0
1-3 / 1-6	0.0	0.0	0.0	0.0
1-4 / 1-5	0.0	0.0	0.0	0.0

Table 18 Damage figures for connection type 1 of the bottom flange before the end of 2050 (after reinforcement, after burr grinding).

It is noted that in 2018 and 2019 preventive reinforcements were carried out at some locations are / become. This concerns the following locations:

- HRB west 1-2 and 1-7 (both bridges) (2018)
- PRB west 1-2 and 1-7 (both bridges) (2018)
- HRB eastern 1-7 (2 E aanbrug) (2019)
- PRB western 1-1 (1 e aanbrug) (2019)
- PRB west 1-8 (1 e aanbrug) (2019)
- PRB west 1-8 (2 E aanbrug) (2019)

Since the existing welds have not been completely removed during the preventive reinforcement also serve these welds have to be ground and re-welded.

4.2 Type 2: Riveted joints in section sections of the bridge

For the riveted connection at the location of the section divisions, it is checked whether it is with the earlier said reinforcement of the lower flange is possible without replacing the current rivets keep damage below D = 1.0 by the end of 2050. The current damage (at the end of 2018) is shown in Table 19.

$\gamma_{Mf} = 1.35$	**HRB west**	**HRB east**	**PRB west**	**PRB east**
Year	**2018**	**2018**	**2018**	**2018**
2-1	0.3	0.1	0.3	0.0
2-2	0.5	0.2	0.5	0.0
2-3	0.5	0.3	0.4	0.0
2-4	0.4	0.2	0.4	0.0

Table 19 Damage figures for the type 2 connection until the end of 2018 (for reinforcement).

For the normative HRB west, it therefore holds that for connection 2-2 and 2-3 a maximum of D = 0.5 damage may occur.

For the reinforced situation, the damage between now and the end of 2050 has been recalculated with the adjusted SCIA model. The starting point is that there is also a recess in the body of the reinforcement in the section divisions is necessary, because welding on the lap plate will be difficult due to the rivets present. This is based on a height of 50 mm.

Figure 22 Side view connection T-piece on coupling plates at section division in the bottom flange

The fatigue calculation of the reinforced situation was performed with detail category $\Delta\sigma_c = 80$, with slope $m_1 = 5$, equal to the current situation, assuming the net cross-section, inclusive recess in the body of the reinforcement.

The additional damage is shown in Table 20.

$\gamma_{Mf} = 1.35$	HRB west	HRB east	PRB west	PRB east
Year	**2018-2050**	**2018-2050**	**2018-2050**	**2018-2050**
2-1	0.0	0.0	0.0	0.0
2-2	0.0	0.0	0.0	0.0
2-3	0.0	0.0	0.0	0.0
2-4	0.0	0.0	0.0	0.0

Table 20 Damage figures for the Type 2 connection at the end of 2018 (before reinforcement) until the end of 2050 (after reinforcement).

It can be seen that no additional damage occurs. The total damage at the end of 2050 will therefore be equal to shown in table in Table 19. Thus, it is not necessary to replace the rivets in the joint to take away the current damage.

4.3 Type 3: Vertical pleat stiffeners inside - weld with bottom flange of the main beams

For many connections of the vertical pleat stiffeners on the inside of the main beam with the lower flange of the main beam, these do not currently meet the damage requirement D < 1.0. The damage will therefore have to be removed first by applying burr grinding to the lasteen (shown in red).

Figure 23 Weld type 3 (shown in red)

Given the throat diameter of the weld (a = 4 mm), after the damage has been worn away, the weld will need to be laid again. The starting point is that the weld must first be laid again, before grinding the next cross stiffener (between two K-bandages). Can be considered then burr grind again to increase the detail category. The damage to it end of 2050, taking into account the reinforced cross-section and the removal of the current one damage, can then be determined on the basis of detail category $\Delta\sigma_c$ = 80x1.3 = 104, see Table 21. Herewith based on the normative detail 3-11.

γ_{Mf} = 1.35	HRB west	HRB east	PRB west	PRB east
Year	2050	2050	2050	2050
3-11	0.0	0.0	0.0	0.0

Table 21 Damage figures for compound 3-11 before the end of 2050 (after reinforcement, with burr grinding) DC = 104.

As can be seen, no new damage occurs in the joint after reinforcing the cross section. Also is it is possible not to re-burr the expanded weld. Calculations must then be made with the original detail category $\Delta\sigma_c$ = 80, although the damage starts at D = 0.0 and may be calculated with the reduced voltage change by adding the tee. Table 22 gives the damage numbers for this situation.

γ_{Mf} = 1.35	HRB west	HRB east	PRB west	PRB east
Year	2050	2050	2050	2050
3-1	0.0	0.0	0.0	0.0
3-2	0.0	0.0	0.0	0.0
3-3	0.4	0.0	0.2	0.0
3-4	0.2	0.0	0.1	0.0
3-5	0.1	0.0	0.1	0.0
3-6	0.0	0.0	0.0	0.0
3-7	0.0	0.0	0.0	0.0
3-8	0.2	0.0	0.1	0.0

3-9	0.0	0.0	0.0	0.0
3-10	0.0	0.0	0.0	0.0
3-11	0.1	0.0	0.1	0.0
3-12	0.1	0.0	0.1	0.0

Table 22 Damage numbers of compound 3-11 before the end of 2050 (after amplification), DC = 80.

Given the limited increase, it is decided not to apply burr grinding after the removal of the weld. For a full description of the steps to be performed, see report T & P-BF7387-R011.

The table below shows the damage at the end of 2018 and the end of 2050. The cells with a white background are the details that in principle do not need to be addressed, because the damage at the end of 2050 will be below 1.0 remains. The cells with a red background in 2018 correspond to the details where burr grinding should be are applied. The details with damage D ≥ 0.9 (shown in orange) at the end of 2018 should be used also to be included, because it will be several years before the reinforcements will take place to be realised.

γ_{Mf} = 1.35	HRB west		HRB east		PRB west		PRB east	
Year	2018	2050	2018	2050	2018	2050	2018	2050
3-1	0.5	0.5	0.3	0.3	0.4	0.4	0.0	0.0
3-2	0.9	0.0 [1]	0.5	0.5	0.9	0.0 [1]	0.0	0.0
3-3	1.9	0.4 [1]	1.0	0.0 [1]	1.8	0.2 [1]	0.1	0.1
3-4	1.9	0.2 [1]	1.0	0.0 [1]	1.8	0.1 [1]	0.1	0.1
3-5	1.4	0.1 [1]	0.7	0.7	1.4	0.1 [1]	0.1	0.1
3-6	1.9	0.0 [1]	1.0	0.0 [1]	1.9	0.0 [1]	0.1	0.1
3-7	0.2	0.2	0.1	0.1	0.2	0.2	0.0	0.0
3-8	0.1	0.3	0.0	0.0	0.1	0.2	0.0	0.0
3-9	0.2	0.2	0.1	0.1	0.2	0.2	0.0	0.0
3-10	1.5	0.0 [1]	1.0	0.0 [1]	1.5	0.0 [1]	0.1	0.1
3-11	2.6	0.1 [1]	1.6	0.0 [1]	2.6	0.1 [1]	0.2	0.2
3-12	2.5	0.1 [1]	1.5	0.0 [1]	2.5	0.1 [1]	0.2	0.2

[1] Damage in 2050 after application of burr grinding during the renovation

Table 23 Damage figures for connection type 3 before the end of 2018 (before reinforcement) and at the end of 2050 (after reinforcement)

4.4 Type 4: Riveted crossbeam connection to the main beams

As described in section 2.4, we will first examine to what extent it is possible to do without it replacing the rivets and the connection between the bottom flange and the bottom edge of the transverse bracing, but with the reinforced bottom flange, it is possible to reduce the damage by the end of 2050 under the D = 1.0. Both the damage so far and the future damage has been calculated with detail category $\Delta\sigma_c$ = 101, healing m_1 = 4.45 and m_2 = 6.45. For the future damage, the reinforced one is assumed situation. The damage figures are shown in Table 24 for the end of 2018 and 2050, where for the the first period of the unreinforced situation has been assumed and for the second period of the fortified situation.

γ_{Mf} = 1.35	HRB west		HRB east		PRB west		PRB east	
Year	2018	2050	2018	2050	2018	2050	2018	2050
4-1	0.1	0.1	0.0	0.0	0.1	0.1	0.0	0.0
4-2	0.3	0.3	0.1	0.1	0.2	0.2	0.0	0.0
4-3	0.3	0.3	0.1	0.1	0.3	0.3	0.0	0.0
4-4	0.0	0.0	0.0	0.0	0.0	0.0	0.0	0.0
4-5	0.2	0.2	0.1	0.1	0.2	0.2	0.0	0.0
4-6	0.5	0.5	0.2	0.2	0.4	0.4	0.0	0.0
4-7	0.2	0.2	0.1	0.1	0.2	0.2	0.0	0.0

4-8	0.0	0.0	0.0	0.0	0.0	0.0	0.0	0.0

Table 24 Damage figures for connection type 4 before the end of 2018 (before reinforcement) and at the end of 2050 (after reinforcement).

So no more damage is caused by the reinforcement. It is therefore not necessary to replace the rivets.

4.5 Type 5: Welded joints in the section sections of the bridge

4.5.1 V-weld bottom flange

Field 1 and field 3

Existing weld

As described in section 2 .5 is the connection for 5-1 and 5-2 is not possible for the retail category of the connection, because the root of the weld in the thickening plate is not accessible. A possible approach could be to consider the lower flange plate as lost and for the top flange plate to apply burr grinding to the top. The bottom of the top flange plate can then be considered with detail category 112 (flat-ground side V-seam), where from 2018, a reduced tension can be maintained by the tee. The top can then are considered with detail category 71x1.3 = 92.3. In theory, this can do the necessary residual lifespan of 30 years can be achieved.

However, TNO has conducted research into the influence of welding imperfections on the fatigue life span. From this it followed that for detail 5-2 there was still a covering in some locations is necessary. In consultation with Rijkswaterstaat, it has been decided for details 5-1 and 5-2 for HRB west, HRB east and PRB west nevertheless apply an overhang to avoid any uncertainties with regard to this to eliminate the welding imperfections.

Strengthening

For these connections, therefore, an enclosure has been designed that has the function of the original welding will take over if they fail. For the enclosure are both top and bottom the current lower flange uses two strips, which are connected by means of preload injection bolts. Any cross stiffeners that get in the way must be shortened and through to be connected to one of the bias injection bolts by means of an angle iron.

Figure 24 V-seam housing existing bottom flange

The surface of the existing flanges and the coupling plates must be blasted and provided of ethyl zinc silicate, so that a minimum friction factor of μ = 0.4 is achieved. For the fatigue calculations are based on detail category 112, in accordance with detail 8 of Table 8.1 of NEN-EN 1993-1-9.

Figure 25 Detail category of prestressed injection bolt connection

The prestressed injection bolt connection is based on the gross cross section of the bottom flange, excluding the top plates. The following damage figures follow from the damage calculation.

$\gamma_{Mf} = 1.35$	HRB west	HRB east	PRB west	PRB east
Year	2050	2050	2050	2050
5-1	0.0	0.0	0.0	0.0
5-2	0.0	0.0	0.0	0.0

Table 25 Damage figures at the location of the prestressed injection bolt connection at the end of 2050 (after reinforcement), first and third field, DC = 112.

Burr grinding existing welds

It should be noted that the outer sides of the V-seams also need to be burr gravel to cover them ensure that only the root of the bottom V-seam remains critical and therefore only the thickening plate in the in the future. To prevent a possible crack in the bottom cover plate grow, the flank joint between the two flange plates of the original main beam should be removed over approx. 100 mm length (shown in blue in the figure below). For the full description of the steps to be taken, please refer to report T & P-BF7387-R011.

Figure 26 Location of weld to be removed between bottom flange and thickener plate (shown in blue) and weld to grind (red displayed)

By removing the longitudinal weld, a new location with a lower detail category is created. The detail category of the interrupted longitudinal weld can be used as detail category 80, conform detail 8 of Table 8.2 of NEN-EN 1993-1-9. This is therefore normative above the detail category of the pre-stressed injection bolt connection.

Figure 27 Detail category for interrupted fillet welds in the longitudinal direction

The damage figures are shown in Table 26 . The cross-section properties have been taken into account that the bottom bulkhead no longer cooperates constructively and that there is a recess in the body of the T-piece is present. However, on the top and bottom of the existing bottom flange there are 4 strips of the housing available (160x30 mm), which can transfer the power. The connection in the PRB east in principle also without reinforcement and therefore does not have to be over-safe.

$\gamma_{Mf} = 1.35$	HRB west	HRB east	PRB west	PRB east
Year	**2050**	**2050**	**2050**	**2050**
5-1	0.0	0.0	0.0	0.0
5-2	0.0	0.0	0.0	0.0

Table 26 Damage figures at the location of the prestressed injection bolt connection at the end of 2050 (after reinforcement), first and third field, DC = 80.

Field 2

In the second field, no rebate plate is used in the bottom flange of the main girders and can therefore, besides the reinforcement with the T-profile, burr grinding can be applied instead of overcutting the weld. This can bring the damage back to D = 0.0 (to be checked by means of NDT).

Figure 28 Burr grinding of the weld type 5-3

The connection has therefore been tested for detail category of $\Delta\sigma_c = 71 * 1.3 = 92.3$. For the tension in the lower flange takes into account a surcharge of 28 mm / (28 mm - 2 mm) = 1.08 in connection with the decrease in thickness. Table 27 shows the test results.

$\gamma_{Mf} = 1.35$	HRB west	HRB east	PRB west	PRB east
Year	**2050**	**2050**	**2050**	**2050**
5-3	0.0	0.0	0.0	0.0

Table 27 Damage numbers in the V weld in the lower flange before the end of 2050 (after reinforcement, after burr grinding), second field, DC = 92.3.

In principle, the weld in the PRB East does not need to be tackled, it also has one without burr grinding damage $D \leq 1.0$.

4.5.2 X-welded body

The main beams' web plates are connected by an X-weld in the same locations as the v-welding in the bottom flange. To eliminate the current fatigue damage in the joints, burr grinding applied. Burr grinding should be applied on both sides of the X-weld to avoid damage at the toe of the weld, see Figure 29 , after which this should be checked by means from NDT. It is believed that 2mm per side is burr gravel to remove the damage, then the weld is sealed again, after which in a second milling pass 1 mm burr gravel, with a tolerance of +/- 0.5 mm. This will reduce the thickness of the body (locally) to a maximum of 9 mm. For the full description of the steps to be taken please refer to report T & P-BF7387-R011.

Figure 29 Burr grinding of the X-weld in the body.

First of all, it was examined at what level the damage would be without burr grinding, taking into account with the reinforcement with the T-piece for the period after 2018. To keep some reserve for the damage development in the time between now and the actual implementation, the height at which the damage D ≤ 0.8 is without burr grinding.

$\gamma_{Mf} = 1.35$	HRB west		HRB east		PRB west		PRB east	
Year	**2018**	**2050**	**2018**	**2050**	**2018**	**2050**	**2018**	**2050**
5-1 (0 mm)	0.6	0.7	0.3	0.3	0.5	0.6	0.0	0.1
5-2 (200 mm)	0.6	0.6	0.3	0.3	0.6	0.6	0.0	0.1
5-3 (300 mm)	0.8	0.8	0.5	0.5	0.8	0.8	0.0	0.1

Table 28 Damage figures in the body for the indicated height of the Type 5 connection before the end of 2018 (for reinforcement) and at the end of 2050 (after reinforcement, without burr grinding).

The weld in the body at connection 5-1 therefore does not have to be burr gravel. The connections 5-2 in the western beams of the HRB and PRB, gravel must be buried over 200 mm and the connections 5-3 in the HRB west and east and PRB west over 300 mm.

For the situation after burr grinding, a detail category DC = 90 * 1.30 = 117 ≤ can be assumed 112 => 112. The damage may also be maintained at D = 0.0, because the current damage will be deleted. However, the body thickness decreases to a maximum of 9 mm, which will result in a stress surcharge of 12 mm / 9 mm = 1.33, but on the other hand the voltage change decreases again by adding of the tee. Based on these principles, the damage has been re-determined for the locations where must be grind.

$\gamma_{Mf} = 1.35$	HRB west	HRB east	PRB west	PRB east
Year	**2050**	**2050**	**2050**	**2050**
5-2	0.0	0.0	0.0	0.0
5-3	0.0	0.0	0.0	0.0

Table 29 Damage figures of connection type 5 (bottom of body) before the end of 2018 (before reinforcement) and at the end of 2050 (after reinforcement, with burr griding).

4.6 Type 6: Flank seal between the cover plate and the bottom flange

The cover plates in the bottom flange are welded to the bottom flange with a flange weld. For this connection is looked at the extent to which the connection is sufficient, with the period from now until the end of 2050 being assumed of the voltage fluctuations in the amplified situation. This is based on detail category 100. The damage calculation results are shown in Table 30.

$\gamma_{Mf} = 1.35$	HRB west		HRB east		PRB west		PRB east	
Year	**2018**	**2050**	**2018**	**2050**	**2018**	**2050**	**2018**	**2050**
6-1	0.3	0.3	0.2	0.2	0.3	0.3	0.0	0.0
6-2	0.8	0.8	0.3	0.3	0.7	0.7	0.0	0.0
6-3	0.8	0.8	0.4	0.4	0.7	0.7	0.0	0.0
6-4	0.5	0.5	0.2	0.2	0.5	0.5	0.0	0.0
6-5	0.0	0.0	0.0	0.0	0.0	0.0	0.0	0.0

Table 30 Damage figures in connection Type 6 before the end of 2018 (without reinforcement) and at the end of 2050 (with reinforcement), DC = 100.

The calculation shows that no additional damage occurs, so the damage is equal to the current damage remains.

4.7 Type 7, 10, 11 and 12 - Cross beam - main beam connection

Fatigue of the connection between the cross beam and the main beam / cross stiffener web not yet tested. Additional research (strain measurements) is currently being carried out for this. The results of these measurements and the testing of fatigue will be made in a later version of this reports are added.

4.8 Type 13: Flank weld between the web and the lower flange of the main beam

For the flank weld between body and bottom flange, the damage until 2018 is without reinforcement and between 2018 and 2050 determined with reinforcement and shown in Table 31. It can be seen that there is only for the western main girders at compound 13-3 is an increase in damage in the last period of ΔD = 0.1.

$\gamma_{Mf} = 1.35$	HRB west		HRB east		PRB west		PRB east	
Year	**2018**	**2050**	**2018**	**2050**	**2018**	**2050**	**2018**	**2050**
13-1	0.1	0.1	0.1	0.1	0.1	0.1	0.0	0.0
13-2	0.3	0.3	0.2	0.2	0.3	0.3	0.0	0.0

13-3	0.8	0.9	0.3	0.3	0.7	0.8	0.0	0.0
13-4	0.8	0.8	0.4	0.4	0.7	0.7	0.0	0.0
13-5	0.5	0.5	0.2	0.2	0.5	0.5	0.0	0.0
13-6	0.8	0.8	0.4	0.4	0.8	0.8	0.0	0.0
13-7	0.0	0.0	0.0	0.0	0.0	0.0	0.0	0.0
13-8	0.0	0.0	0.0	0.0	0.0	0.0	0.0	0.0
13-9	0.1	0.1	0.0	0.0	0.0	0.0	0.0	0.0
13-10	0.6	0.6	0.4	0.4	0.5	0.5	0.0	0.0
13-11	1.1	1.1	0.7	0.7	1.1	1.1	0.1	0.1
13-12	1.1	1.1	0.6	0.6	1.0	1.0	0.1	0.1

Table 31 Damage figures in connection Type 13 for the end of 2018 and the end of 2050, DC = 100.

From the results it becomes clear that after the installation of the extra profile under the bridge there is hardly any fatigue damage is added in this detail. This, in combination with the very limited exceeding of the fatigue life and additional complexity of replacing this weld makes that for this detail physical reinforcement measures would be disproportionate. It is therefore recommended to use the weld 13-3, 13-11 and 13-12 on the western girders with NDT to crack inspect. For a full description of the research to be carried out, please refer to the report T & P-BF7387-R011.

4.9 Type 14: Cross stiffener - longitudinal stiffener - bulkhead connection end cross member

From the fatigue calculation of the welded connection between the cross stiffener, the bulkhead and the longitudinal stiffener at the location of the portal of the end bearings has shown that the welds in the flange on the inside of the portal and in the body are not satisfactory. The weld connection in the flange on the exterior is just not enough in the verification calculation, but there is still some conservatism. Here is discussed in detail 14D.

Figure 30 Connection between transverse stiffener, longitudinal stiffener and the bulkhead under the transverse beam at the end support point

The reinforcement consists of replacing the welds for a different type of weld, which is no longer welding root has. The following numbering is used.

- Detail 14A: Weld connection between the flange of the transverse stiffener (inside of bridge) with the flange of the longitudinal stiffener (bulb)
- Detail 14B: Weld connection between the body of the transverse stiffener and the body of the longitudinal stiffener and welding connection between the bulkhead and the body of the longitudinal stiffener
- Detail 14C: x-weld between flange bulkhead and flange of the longitudinal stiffener (bulb)
- Detail 14D: Weld connection between the flange of the cross stiffener (outside of bridge bridge) with the flange of the bulkhead

For each detail, the following sections explain whether and how the detail is adjusted and how results of the fatigue calculation.

Detail 14-A: Weld connection transverse stiffener flange - longitudinal stiffener flange

The weld between the flange of the transverse stiffener and the flange of the longitudinal stiffener (bulb) is recalculation not on the root test. The measurements also showed that the voltages are too be high to meet the damage claim. The results show that the damage is so high that it is necessary to come up with a solution with a weld where there is no longer a root. It has been decided to mill away a part of the bulb and replace it for a full penetration, see detail 14-A.

Weld and share bulb
mill away

Figure 31 Current situation (left) and modified weld (right) at detail 14-A

The detail can be considered as a V-weld, with a detail category 71 according to detail 13 in table 8.3 of NEN-EN 1993-1-9. However, the weld is eccentric, so there is actually an extra voltage concentration factor must be included.

In the measurements, the hot spot voltage at the location of the original weld was measured at the outside of the flange. The voltage concentration has therefore already been included in this measurement. The new read (V-weld) is slightly different in geometry from the original weld (incomplete V-weld a = 6 mm plus one sealing weld a = 3 mm). Given the geometry, the new weld will be less high have a voltage concentration factor relative to the original weld. Therefore, there can be for the fatigue calculation can still be counted conservatively with the reduced influence lines on based on the relationship between the measured stresses and the calculated stresses. Furthermore, it is assumed that the voltage (change) in this connection will not change significantly by strengthening the main beam.

The detail category that can be used for a hotspot analysis is generally higher than the detail category for nominal voltages. However, there is none in Appendix B of NEN-EN 1993-1-9 detail category given for the proposed weld. In all likelihood, the detail category will be approx. 90 to 100. For example, a cross weld has a detail category of 100 in a hotspot analysis. For the however, it has been decided to use detail category 71 conservatively, as given for rated voltages. So this is conservative.

Weld toe fatigue analysis was performed for three partial safety factors, where the damage has been determined before the end of 2050. The basic principle is that the damage will be removed by replacement of the weld, so that the damage returns to zero after replacing the weld. The results are summarized in the following table.

	HRB west	HRB east	PRB west	PRB east
γ_{Mf}	2050	2050	2050	2050
1.35	0.1	0.0	0.1	0.0
1.15	0.0	0.0	0.0	0.0
1	0.0	0.0	0.0	0.0

Table 32 Damage figures for the end of 2050 for ½ V weld in the flange (Type 14-A)

The stresses due to permanent loads were approx. 47 N / mm² in the flange for reinforcement. While replacing the weld this voltage will be redistributed to the rest of the cross-section. At the replacing the welds in the body some of these (permanent) stresses will go back to the flange. The level of the permanent stress does not matter for the fatigue analysis (no relevant for testing the toe of the weld). Class 1 applies to the UGT profile, so that any excess stress of the yield stress in one of the parts will result in voltage redistribution. The final capacity will remain the same. A additional UGT testing is therefore not necessary.

Detail 14-B: Weld connection transverse stiffener body - longitudinal stiffener body and bulkhead - longitudinal stiffener body

The fillet welds between the bulkhead and the body of the longitudinal stiffener (including a part on the inside of the flange) and the weld between the body of the cross stiffener and the body of the long stiffener replaced by K-welding.

Read and share

Milling body / bulkhead

Figure 32 Current situation (top) and reinforced situation (bottom) at type 14-B site

The replacement of each weld must be done per side, so first one side of the plate / body, and only then the other side of the plate / body. The existing fillet weld (a = 5) and the plate serve this purpose milled away halfway to the plate, in such a way that it is prepared for a k-weld. After this the plate must be welded again. A weld must be present on at least one side at all times to be. After welding, cross-stiffener must be applied to the toe on the side of the bulkhead / body and a transition should be made to the existing welds over 50 mm.

No reduction from the measurements has been included for the fatigue calculation, because no measurements have been taken to the welded connection in the body. The assessment is based on detail category $\Delta\sigma_c$ = 80 N / mm², based on from detail 1 in table 8.5 of NEN-EN 1993-1-8 (K-weld without gap).

Weld toe fatigue analysis was performed for three partial safety factors, where
the damage has been determined before the end of 2050. The basic principle is that the damage will be removed by replacement
of the weld, so that the damage returns to zero after replacing the weld. The results are summarized in
the following table.

γ_{Mf}	HRB west	HRB east	PRB west	PRB east
	2050	2050	2050	2050
1.35	0.6	0.1	0.3	0.0
1.15	0.3	0.0	0.1	0.0
1	0.1	0.0	0.0	0.0

Table 33 Damage figures for the end of 2050 for K-weld without gap (Type 14-B)

Detail 14-C: Weld connection flange bulkhead - flange longitudinal stiffener
According to the drawing, the X-weld in the flange is not fully welded. Because of this there is
there is also a root of the weld at the top. Just like the weld on the bottom of the
bulb does not comply and must therefore be replaced for full penetration. The splice serves this purpose
milled away and replaced for a butt weld. At the center spot
of the flange this will have to be done from the outside, whereby the new weld is welded to the body / bulkhead
is going to be. Outside the body you can choose to place a counter weld.

Weld and divide flange
mill away

Figure 33 Current situation (left) and modified weld (right) at detail 14-C

No calculation has been performed for this weld, since according to the measurements the voltages in the
flange on the top of the bulb is lower than on the bottom of the bulb.

Detail 14-D: Weld connection flange bulkhead outside - flange cross stiffener

The connection in the flange on the outside just failed in the verification calculation fatigue of the toe of the weld at $\gamma_{Mf} = 1.35$.

Figure 34 Weld connection flange transverse stiffener outside

For the testing of the toe of the weld, the ratio between the measured hotspot voltages and the calculated nominal voltages and has been tested on the basis of detail category 90 (based on detail 7 of Appendix B of NEN-EN 1993-1-1). The following followed damage numbers.

	HRB west		HRB east		PRB west		PRB east	
γ_{Mf}	**2018**	**2050**	**2018**	**2050**	**2018**	**2050**	**2018**	**2050**
1.35	0.4	1.2	0.3	0.6	0.3	0.7	0.1	0.3
1.15	0.1	0.5	0.1	0.2	0.1	0.3	0.1	0.1
1	0.1	0.2	0.0	0.1	0.0	0.1	0.0	0.0

Table 34 Damage figures for the end of 2018 and the end of 2050 for the toe of the weld (type 14-D) based on measurements detail DDE-L (hotspot)

For testing the root of the weld, the ratio between the measurements was taken into account nominal voltages and the calculated nominal voltages and has been tested on the basis of detail category 71, as determined in consultation with TNO. This resulted in the following damage numbers.

	HRB west		HRB east		PRB west		PRB east	
γ_{Mf}	**2018**	**2050**	**2018**	**2050**	**2018**	**2050**	**2018**	**2050**
1.35	0.1	0.4	0.1	0.2	0.1	0.2	0.0	0.1
1.15	0.0	0.1	0.0	0.0	0.0	0.1	0.0	0.0
1	0.0	0.0	0.0	0.0	0.0	0.0	0.0	0.0

Table 35 Damage figures for the end of 2018 and the end of 2050 for the root of the weld (type 14-E) based on measurements detail DDE-L (nominal)

However, it was noted that the lower traffic spectrum had not yet been taken into account, as determined by TNO in report TNO-2019-R11393 [5], TNO-2019-R11394 [6] and TNO-2020-R10226 [8]. If this were taken into account, it can be assumed that the toe of the weld does meet fatigue. So there is no need to adapt to the weld on the outside turn into.

4.10 Type 15: Cross stiffener - longitudinal stiffener - bulkhead connection intermediate support

At the location of the intermediate supports, a comparable one is located on the inside of the main beam connection present between the bulkhead under the cross beam, the longitudinal stiffener and the transverse stiffener as at the end impositions. Here too, the connection is not sufficient for fatigue in the recalculation. Chosen is here to perform the reinforcement in the same manner as for the end cross member.

Figure 35 Connection between transverse stiffener, longitudinal stiffener and the bulkhead under the transverse beam at the intermediate support point

The reinforcement consists of replacing the welds for a different type of weld, which is no longer welding root has. The following numbering is used.

- Detail 15A: Weld connection between the flange of the transverse stiffener (inside of bridge) with the flange of the longitudinal stiffener (bulb)
- Detail 15B: Weld connection between the body of the transverse stiffener and the body of the longitudinal stiffener and welding connection between the bulkhead and the body of the longitudinal stiffener
- Detail 15C: x-weld between flange bulkhead and flange of the longitudinal stiffener (bulb)

For each detail, the following sections explain whether and how the detail is adjusted and how results of the fatigue calculation.

Detail 15-A: Weld connection transverse stiffener flange - longitudinal stiffener flange

Reinforcement is performed in the same manner as for Type 14-A, with full penetration is realized with V-weld, see section 4.10.

Weld and share bulb
mill away

Figure 36 Current situation (left) and modified weld (right) at detail 15-A

As with type 14-A, a detail category 71 becomes in accordance with detail 13 in table 8.3 of NEN-EN 1993-1-9
apprehended. The measured values are taken into account for voltage fluctuations
hotspot voltages, as described in TNO report TNO-2019-R11393 [5], where it is determined that the
stresses are 74% of the calculated stresses. It is assumed that the voltage (alternation) is in
this connection will not change significantly due to the reinforcement of the main beam.

Weld toe fatigue analysis was performed for three partial safety factors, where
the damage was determined before the end of 2050. The results are summarized in the table below.

γ_{Mf}	HRB west	HRB east	PRB west	PRB east
	2050	2050	2050	2050
1.35	0.6	0.0	0.3	0.0
1.15	0.2	0.0	0.1	0.0
1	0.1	0.0	0.1	0.0

Table 36 Damage figures for the end of 2050 for ½ V weld in the flange (Type 15-A)

Detail 15-B: Weld connection transverse stiffener body - longitudinal stiffener body and bulkhead - longitudinal stiffener body

The fillet welds between the bulkhead and the body of the longitudinal stiffener (including a part on the inside
of the flange) and the weld between the body of the cross stiffener and the body of the long stiffener
replaced by K-welding.

Read and share
Milling body / bulkhead

Figure 37 Current situation (left) and reinforced situation (right) at type 15B site

The method of replacement is described for type 14-B, see section 4.10.

The replacement of each weld must be done per side, so first one side of the plate / body,
and only then the other side of the plate / body. The existing fillet weld (a = 4) and the plate serve this purpose
milled away halfway to the plate, in such a way that it is prepared for a k-weld. After this
the plate must be welded again. A weld must be present on at least one side at all times
to be.

After welding, cross-stiffener must be applied to the toe on the side of the bulkhead / body
turn into.

The reduction from the measurements was not included for the fatigue calculation, because the measurement results gave a different picture. It follows from the fatigue calculation that the weld is not satisfactory without improving the weld. Therefore, it should be on the toe of the weld on the side of the bulkhead and the body of the transverse stiffener burr grinding to be applied to increase fatigue strength. Compliant IIW [9] may assume a 30% increase in the detail category. Based on a k-weld ($\Delta\sigma_c$ = 80) and 30% increase in the detail category, the connection is calculated at $\Delta\sigma_c$ = 104 N / mm².

Weld toe fatigue analysis was performed for three partial safety factors, where the damage has been determined before the end of 2050. The basic principle is that the damage will be removed by replacement of the weld, so that the damage returns to zero after replacing the weld. The results are summarized in the following table.

γ_{Mf}	HRB west	HRB east	PRB west	PRB east
	2050	2050	2050	2050
1.35	0.4	0.0	0.2	0.0
1.15	0.2	0.0	0.1	0.0
1	0.0	0.0	0.0	0.0

Table 37 Damage figures for the end of 2050 for K-weld web (Type 15-B)

Detail 15-C: Weld connection flange bulkhead - flange longitudinal stiffener

According to the drawing, the X-weld in the flange is not fully welded. Because of this there is there is also a root of the weld at the top. Just like the weld on the bottom of the bulb not compliant and must therefore be replaced for full penetration (butt weld). For this the same reinforcement as type 14-C is assumed, see section 4.10 .

Weld and share bulb
mill away

Figure 38 Part to be removed (shown in red) and part to be welded on top of bulb

No calculation has been performed for this weld, since according to the measurements the voltages in the flange on the top of the bulb is lower than on the bottom of the bulb.

4.11 Type 16: Connection cross-stiffener - bulkhead cross-members

It follows from the recalculation that the (nominal) voltage fluctuations at the location of the others cross bars are very limited. This will not change significantly in the reinforced situation. There will therefore no damage to these connections.

4.12 Type 17: Vertical pleat stiffeners - weld with main beam web

For a large number of connections between the body of the vertical pleat stiffeners and the body of the the main girder applies that they currently do not meet the damage requirement D <1.0. So the damage will must first be removed by applying burr grinding to the welding stone (blue displayed). For a description of the complete procedure, reference is made to report T & P-BF7387-R011.

Figure 39 Reinforced connection between cross stiffener body and main beam body (shown in blue).

For the situation after burr grinding, the original detail category $\Delta\sigma_{c\ \mathrm{was}}$ initially used = 80, where the damage starts at D = 0.0 and may be counted with the reduced voltage change by adding the T-piece. This followed from the calculations of type 3 HRB West will incur a maximum of 0.1 damage.

The table below shows the damage at the end of 2018. The cells with a white background are the details which in principle do not need to be addressed, because the current damage is D ≤ 0.8 and therefore maximum 0.1 is added, keeping the damage below D = 1.0. The other welds (cells with red background) need to be addressed.

γ_{Mf} = 1.35	HRB west	HRB east	PRB west	PRB east
Year	**2018**	**2018**	**2018**	**2018**
17-1	0.4	0.3	0.4	0.0
17-2	0.7	0.4	0.7	0.0
17-3	1.5	0.8	1.5	0.1
17-4	1.5	0.8	1.5	0.1
17-5	1.1	0.5	1.1	0.0
17-6	1.7	0.8	1.7	0.1
17-7	0.1	0.0	0.1	0.0
17-8	0.1	0.0	0.1	0.0
17-9	0.2	0.1	0.1	0.0
17-10	1.3	0.8	1.3	0.1
17-11	2.2	1.4	2.2	0.2
17-12	2.2	1.2	2.2	0.1

Table 38 Damage figures for type 17 connection before the end of 2018

To determine the height to which burr grinding should be applied, the height at which the current damage falls below D = 0.8. The height is measured from the bottom of the existing one bottom flange.

γ_{Mf} = 1.35	Height from / to	HRB west	HRB east	PRB west
Year	**underside**	**2018**	**2018**	**2018**
17-3	400	0.7		0.7
17-4	400	0.7		0.7
17-5	300	0.7		0.7
17-6	400	0.8		0.8
17-10	300	0.8		0.7
17-11	500	0.8	0.5	0.8
17-12	500	0.8	0.4	0.8

Table 39 Height at which damage D ≤ 0.8 of type 17 connection before the end of 2018

The starting point for burr grinding is a depth of 1.0 mm +/- 0.5 mm on one side. The body thickness is possible so decrease from 12 mm to 10.5 mm. On the other hand there is an improvement of the detail category (1.3 * 80 = 104). Since the detail also satisfied a detail category 80, without decreasing the thickness of the body (D <0,1), it can be assumed that this detail also suffices after burr grinding. The decrease of the thickness (14%) more than outweighs the increase in the detail category (30%).

4.13 Type 20: Weld connection at the location of the recess in the body of the tee

The main beams of the bridges are reinforced with an inverted T-piece to reduce the stresses in the reduce the lower flange of the main beam. At the location of the welds at the ends of the reinforcement plates (type 1, detail 1), the riveted joints (type 2, detail 2) and at the location of the V-seams which are vaulted (type 5, detail 3) a recess is made on the top of the body, because this connection is otherwise difficult to realize and / or to be able to use the (existing) connections inspect, see Figure 40 .

Figure 40 Geometry of the recesses in the body of the T profile

The connection is tested at the locations at the end of the thickening plates (20-1, 20-4, 20-6 and 20-7), at the location of the section divisions (20-5, 20-8) and at the location of the V-seam being covered (20-2 and 20-3) in the outer fields.

20-3 20-4 20-5 20-6

20-1 20-2

20-7 20-8

Figure 41 Location of the recesses in the body of the T profile

For the recesses in the body with height less than 60 mm in accordance with NEN-EN 1993-1-9 detail category 71 maintained, see Figure 42.

Figure 42. The detail category of a recess in the body, detail 9 Table 8.2 of NEN-EN 1993-1-9.

However, the literature shows that the fatigue strength of this type of cut-out is influenced by the height of the shear stress in the body. The effect of the shear stress in the body is described in the IIW report Recommendations for fatigue design of welded joints and components [9] included for the determine the detail category, see Figure 43 . The detail category depends on the ratio between the shear stress in the web and normal stress in the bottom flange.

Figure 43 Detail category at the location of a recess as a function of the shear and normal stress [9]

The ratio of the shear stress in the web and the normal stress in the (existing) bottom flange is determined for the UGT taxes for the normative detail closest to the imposition (20-6). The shear force for this cut is approx. 1200 kN, resulting in a shear stress of approx. 42 N / mm². The tension in the (existing) bottom flange is approx. 200 N / mm² in the UGT. This brings up the relationship 0.21, resulting in a detail category $\Delta\sigma_c$ = 56 N / mm². This is a conservative assumption because it maximum moment does not in principle occur simultaneously with the maximum transverse force. For connection 20-3 and 20-4, the ratio will certainly be below 0.2 and is based on $\Delta\sigma_c$ = 63 N / mm². With this conservative assumption, all connections were initially calculated. The test results are shown in Table 40 .

γ_{Mf} = 1.35	HRB west	HRB east	PRB west	PRB east
Year	**2050**	**2050**	**2050**	**2050**
20-1	0.4	0.0	0.2	0.0
20-2	0.6	0.0	0.3	0.0
20-3	0.6	0.0	0.3	0.0
20-4	1.3	0.1	0.7	0.0
20-5	0.1	0.0	0.0	0.0
20-6	0.1	0.0	0.0	0.0

20-7	0.1	0.0	0.1	0.0
20-8	0.1	0.0	0.0	0.0

Table 40 Damage figures for compound type 20 before the end of 2050.

Connection 20-4 does not meet the damage requirement D ≤ 1.0 for the western beam of the HRB.
However, the above-mentioned detail category is conservative because it has not been taken into account that all gates with a reinforced weld (full penetration) at the end are performed, similar to detail 3 in accordance with table 8-4 of NEN-EN 1993-1-9. This requires a smooth transition curve be realized by machining the gusset plate prior to welding and by welding zone (shown in dotted lines in Figure 44 Principle of body rounding at the location of welding gates Figure 44) to be sharpened with a burr parallel to the direction of the span so that the entire weld in transverse direction is removed.

Part to be sharpened

Figure 44 Principle of rounding body at the location of welding gates

The standard does not provide a detail category for such a connection. 30% as an indication improvement, comparable to the improvement in burr grinding according to IIW document [IW-2259-15 [9] . The detail category then becomes 63 * 1.3 = 81.9. Compound 20-4 has therefore been tested again with this one detail category, see Table 41 . This means that the detail meets the fatigue requirement.

γ_{Mf} = 1.35	HRB west	HRB east	PRB west	PRB east
Year	**2050**	**2050**	**2050**	**2050**
20-4	0.3	0.0	0.2	0.0

Table 41 Damage figures of connection type 20-4 before the end of 2050, DC = 81.9.

4.14 Type 21: Welded bulkheads on bottom flange of the T piece

The stability test in section 5.1 .4 has shown that it is necessary to add supports against buckling of the bottom flange sideways. The bulkheads are welded to the bottom flange with a fillet weld and body of the T piece and welded to the lower flange of the main beams, see Figure 45 . Because there in it extension of the transverse stiffener, on the inside of the main beam, a connection under the bottom flange is present with the bottom edge of the k-bandage, the partitions must be on the outside be placed. Above the lower flange there should also be a bulkhead to ensure a rigid connection to the create a transverse stiffener.

Figure 45 Detail of the partitions in the bottom flange T-piece

The detail category is maintained in accordance with NEN-EN 1993-1-9, detail 7 in Table 8.4 and is equal to DC = 80.

Figure 46 Detail category of the welded connection between the bulkhead and bottom flange.

For the fatigue calculation, a test has been performed every 5 m for this detail, so that the exact location can be chosen practically. The locations correspond to type 3. The test results are in Table 42 shown for γ_{Mf} = 1.35.

γ_{Mf} = 1.35	HRB west	HRB east	PRB west	PRB east
Year	2050	2050	2050	2050
21-1	0.0	0.0	0.0	0.0
21-2	0.2	0.0	0.1	0.0
21-3	1.5	0.0	0.7	0.0
21-4	0.5	0.0	0.2	0.0
21-5	0.3	0.0	0.2	0.0
21-6	0.2	0.0	0.1	0.0
21-7	0.0	0.0	0.0	0.0
21-8	0.2	0.0	0.1	0.0
21-9	0.0	0.0	0.0	0.0
21-10	0.2	0.0	0.1	0.0
21-11	0.4	0.0	0.2	0.0
21-12	0.4	0.0	0.2	0.0

Table 422 Damage figures for connection type 21 before the end of 2050, DC = 80

The results show that only at the location of 21-3 in the HRB west does not meet the damage requirement D ≤ 1.0 can be satisfied. If a bulkhead is placed between approx. 13 and 19 m from the end bearing, the toe of the weld should be treated with burr grinding. According to IIW [9] , the fatigue strength of the joint with this treatment improved by 30%, which means the detail category 80 * 1.3 = 104. Compound 21-3 is retested with this detail category and meets the damage requirement D ≤ 1.0.

γ_{Mf} = 1.35	HRB west	HRB east	PRB west	PRB east
Year	2050	2050	2050	2050
21-3	0.4	0.0	0.2	0.0

Table 43 Damage numbers of connection type 21-3 before the end of 2050, DC = 104.

4.15 Type 22: Longitudinal weld between the body and the bottom flange of the T piece

The tee is composed of a web plate and a bottom flange. The connection between the body and the bottom flange of the T-piece is realized with fillet weld a = 7, see Figure 47 (shown in green). The fillet weld with the existing bottom flange is performed as fillet weld a = 5 mm (shown in purple), so that the heat input in the existing construction can be limited. The vertical welds are in discussed in the next section.

Figure 47 Fillet welds between T-piece body and flanges.

According to Table 8.2 of NEN-EN 1993-1-9, the detail category of the longitudinal weld is 100, see Figure 48 .

Figure 48 Detail category of the longitudinal weld in the profile, NEN-EN 1993-1-9.

This fillet weld is tested for fatigue every 5 m. The locations correspond to type 3. Table 44 shows the results of the fatigue calculation. The damage requirement D ≤ 1 is met everywhere.

γ_{Mf} = 1.35	HRB west	HRB east	PRB west	PRB east
Year	**2050**	**2050**	**2050**	**2050**
22-1	0.0	0.0	0.0	0.0
22-2	0.1	0.0	0.0	0.0
22-3	0.7	0.0	0.4	0.0
22-4	0.2	0.0	0.1	0.0
22-5	0.1	0.0	0.1	0.0
22-6	0.1	0.0	0.0	0.0
22-7	0.0	0.0	0.0	0.0
22-8	0.1	0.0	0.0	0.0
22-9	0.0	0.0	0.0	0.0
22-10	0.1	0.0	0.0	0.0
22-11	0.2	0.0	0.1	0.0
22-12	0.2	0.0	0.1	0.0

Table 44 Damage figures for connection type 22 before the end of 2050, DC = 100.

4.16 Type 23: Connection body and flange T piece - X welding

The T-piece will have to be fitted in different parts. In the gain design it is starting point that the different parts of the T-piece are mutually connected by means of a welded joint, see Figure 49 . The butt welds in the body (shown in red) and in the flange (X35) are designed as x-welds that are ground flat in accordance with NEN-EN 1993-1-9 table 8.3 detail 3. Here there is Assume that the weld is first placed in the bottom flange, then a rectangular plate welded into the body with the flanges and the body of the T-piece.

Figure 49 X-seam welded connection between the sections of the T-piece (shown in red in body).

The detail category of an X seam connection is in Table 8.3 of NEN-EN 1993-1-9 detail 3 if DC = 112 in which the effect of the sheet thickness must be included in the calculation. Outgoing for a flange thickness of 35 mm, the detail category DC = 112 * $(25/35)^{0.2}$ is = 105.

Figure 50 The detail category of the X-seam welded joint between the section sections of the tee

The detail category is higher than the detail category that is for the longitudinal weld between body and flange (type 22) held (DC = 100). Since fatigue of the longitudinal weld over the entire length was sufficient, this will be the case also apply to the (flat-ground) x-seam.

4.17 Type 24: Connection end of body tee with existing bottom flange

The body of the tee is terminated with a rounded end of the body plate, see Figure 51 . in addition the width of the flange is chamfered to the end of the flange. This will cause the bottom flange of the tee barely has tension present at the termination of the flange, which is normally one unfavorable detail is for fatigue. Also on the side of the existing bottom flange is due to the rounding created a gradual transition, which is more advantageous from a technical point of view. The fillet weld between body tee and the existing bottom flange is executed over the last part as k-weld instead of two fillet welds. The rounding to the body must be ground flat in a smooth transition, see also report T & P-BF7387-R011. The detail of the termination of the body plate of the tee on the existing bottom flange is tested for fatigue.

Figure 51 Connection end of the T-piece web plate with the bottom flange of the main beam.

This connection occurs at 6 locations per main beam. Due to symmetry, the first three locations are tested.

24-1

24-3

Figure 52 Tested locations, type 24.

For this connection, detail category 80 becomes according to Table 8.4 (detail 3) of NEN-EN 1993-1-9 detained, see Figure 53.

Figure 53 Detail category for connection type 24, NEN-EN 1993-1-9.

The test results are shown in Table 45 before the end of 2050 at γ_{MF} = 1.35. All connections are sufficient to the claim claim D ≤ 1.0.

γ_{Mf} = 1.35	HRB west	HRB east	PRB west	PRB east
Year	**2050**	**2050**	**2050**	**2050**
24-1	0.1	0.0	0.0	0.0
24-2	0.1	0.0	0.1	0.0
24-3	0.2	0.0	0.1	0.0

Table 45 Damage figures for connection type 24 before the end of 2050, DC = 80.

4.18 Type 25: Shear stress welding end of body T-piece

In addition to testing for normal voltage, the flank welds must also be tested for fatigue shear stress changes in the weld. Adding the T-piece will cause more shear stress the existing welds go, especially at the end of the tee. The new welds are also used up shear stress loaded.

Figure 54 Fillet weld between bottom flange and body and between thickening plate and bottom flange

The shear stress will, in particular at the end of the T-piece, at the location of the intermediate support point largest because here the tension in the T-piece must be transferred to the lower flange and the body of the existing main beam. The shear stresses were examined with the aid of a plate model at the location of the different welds. The normal voltage is on the right side of the plate model placed the main beam as a result of the unit load (2x50 kN), to make a translation of the normal stress in the global calculation model to the shear stress at the location of the welds.

The shear stresses (τ_{xy}) at the end of the tee are shown in the figure below.

Figure 55 Shear stresses at the end of the T-piece.

It can be seen that the greatest shear stress peak is in particular at the bottom of the body of the T-piece occurs. At the location of the existing welds, the shear stresses are a lot smaller, but the throat diameter of the welds smaller. The shear stresses are translated into the shear stress in the weld with the formula $\tau_2 = \tau_{xy} * t_w / 2a$. The shear stress in the weld itself remains greatest at the location of the welded connection at the bottom of the tee, despite the larger throat diameter.

The detail category of this connection is maintained in accordance with detail 8 in table 8.5 of NEN-EN 1993-1-9 if DC = 80 with $m_1 = 5$.

Figure 56 Detail category of the welded connection between the web and bottom flange

The calculation was initially performed for the period 2018-2050. It follows that there are virtually no fatigue damage occurs. The locations correspond to type 24.

γ_{Mf} = 1.35	HRB west	HRB east	PRB west	PRB east
Year	2050	2050	2050	2050
25-2	0.0	0.0	0.0	0.0
25-3	0.1	0.0	0.0	0.0

Table 46 Damage figures of connection type 25 for 2018-2050, DC = 80.

For the existing welds in the period before 2018, there is an unreinforced cross-section without tee. The shear stress will therefore have been less during this period. For the period before 2018 it can be assumed that no damage will have occurred.

5 Strength and stability

5.1 Main beam

5.1.1 Calculation approach

The main beam is reinforced over almost the entire length with a T-piece under the existing one bottom flange. As a result, tensions will generally decrease. Therefore, there is an equation made between the voltages before amplification and after amplification. Both the existing bottom flange, as the new bottom flange, because the starting point for the calculation is that this last will only include variable taxes.

In the determination of the stresses, just as in the recalculation, the moments around the weak axis neglected, because they cannot be determined correctly by the finite element model and the local model has shown that these are relatively small (approx. 4 N / mm² for one tandem system of 600 kN). Reference is made to the verification calculation of the existing situation [T & P-BF7387-R005].

It is noted that, due to symmetry, the tandem systems only on the second half of the bridge plus the first intermediate support have been used to save computing time. The tensions in the first half of the bridge must therefore be taken equal to the second half.

5.1.2 Results

In the figures below, the tension in the top flange due to the normal force (N $_{Ed}$) is plus the moment about the strength axis (M $_{y, Ed}$) displayed over the length of the bridge, including the preload at the intermediate support point. In the top figure the original voltage distribution for amplification given, in the bottom figure the voltage after amplification. The tensions are given up usage level, where the red line corresponds to the maximum voltages and the blue line to the minimal stresses.

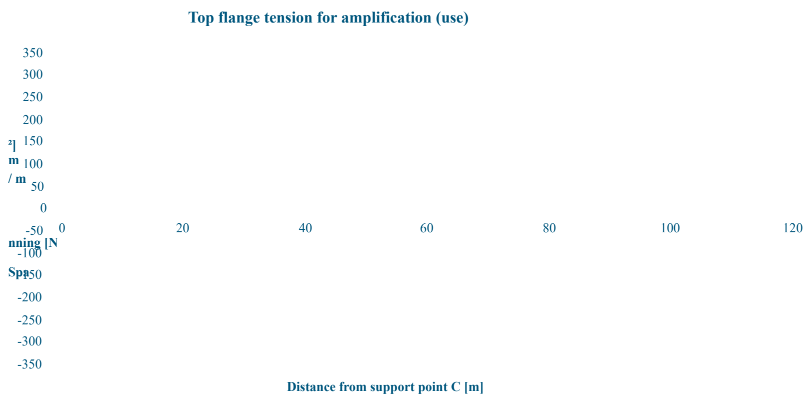

Figure 57 Tensions in the top flange of the main beam for reinforcement due to N $_{Ed}$ + M $_{y, Ed}$ (use)

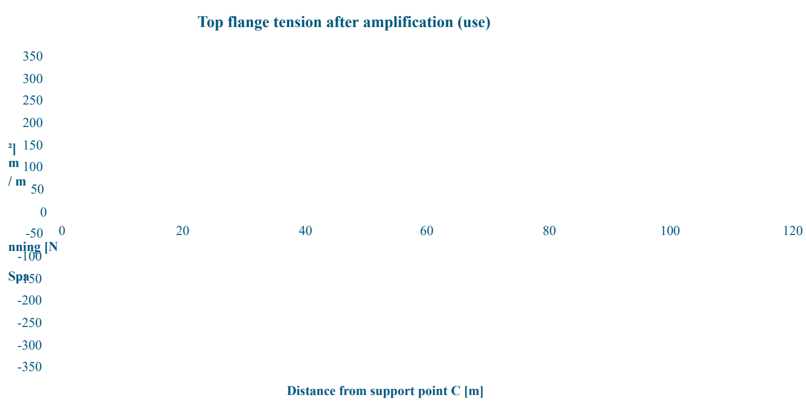

Figure 58 Tensions in the top flange of the main beam after reinforcement due to N $_{Ed}$ + M $_{y, Ed}$ (use)

It can be seen that the stresses in the top flange remain almost the same. This can be explained by the fact that on the one hand, the bending inertia of the main beam has increased (for the variable loads), but on the other hand, the center of gravity of the reinforced cross-section will slide down. Changed on balance the tension little.

The stresses in the original bottom flange are shown in the figures below, again for
the situation before and after reinforcement. Here too, the voltages are shown at the usage level.

Lower flange voltage for amplification (use)

350
300
250
200
²] 150
m 100
/ m 50
0
-50 0 20 40 60 80 100 120
nning [N
-100
Spa-150
-200
-250
-300
-350

Distance from support point C [m]

Figure 59 Stresses in the bottom flange of the main beam for reinforcement due to N_{Ed} + $M_{y, Ed}$ (use)

Lower flange tension after amplification (use)

350
300
250
200
²] 150
m 100
/ m 50
0
-50 0 20 40 60 80 100 120
nning [N
-100
Spa-150
-200
-250
-300
-350

Distance from support point C [m]

Figure 60 Tensions in the original lower flange of the main beam after reinforcement due to N_{Ed} + $M_{y, Ed}$ (use)

For the original bottom flange, it can be seen that the stresses in the field are reduced by approx. 100 N / mm²
taken in fields 2 and 3. At the location of the intermediate support it can be seen that the tension remains the same, because
this part is not reinforced. However, the voltage in the next peak is at the end of the thickening plate
decreased because the gain has moved beyond this point. All tensions remain in the new
situation well below the yield stress (f_y = 350 N / mm²). The greatest stress is found at the (not
reinforced) intermediate support point and equals 318 N / mm².

The tension in the new bottom flange is shown in the figure below. This is based on the tensions at the renovation level, because this is a new part.

T-piece bottom flange tension (rebuild)

350
300
250
200
²]
m 150
/ m 100
50
0
-50 0 20 40 60 80 100 120
nning [N
-100
Spa
-150
-200
-250
-300
-350

Distance from support point C [m]

Figure 61 Tensions in the new bottom flange (T-piece) of the main beam after reinforcement due to N_{Ed} + $M_{y, Ed}$ (conversion)

The stresses in the new bottom flange are up to 120 N / mm², making them well below yield stress (f_y = 355 N / mm²). The wide margin can be explained by the fact that the T-piece only contains the variable load will absorb and the design was needed not so much for strength but more for the reduction of stresses in the original bottom flange for fatigue.

In the figures below, the tension in the top flange of the steel beam is of the individual load components shown along the length of the bridge (without load factor). It the top figure shows the stresses for the non-amplified situation, the bottom one for the situation after strengthening.

Top flange tension for reinforcement

140 Perm. Load (incl. Shrinkage and creep)

120
100
80
60
40
20
0
-20
-40
-60
-80
-100
-120
-140
-160
-180

0 20 40 60 80 100 120

Traffic (including brake load)
Wind F * w
Temperature

²]
m
/ m
panning [N
S

Distance from support point C [m]

Figure 62 Tensions in the top flange of the main beams for reinforcement due to N + M y (per load group)

Top flange tension after reinforcement

140
120
100
80
60
40
20
0
-20
-40
-60
-80
-100
-120
-140
-160
-180

0 20 40 60 80 100 120

Perm. Load (incl. Shrinkage and creep)
Traffic (including brake load)
Wind F * w
Temperature

²]
m
/ m
panning [N
S

Distance from support point C [m]

Figure 63 Tensions in the top flange of the main beams after reinforcement due to N + M y (per load group)

In the figures below, the tension in the lower flange of the steel beam of the individual load components displayed along the length of the bridge (without load factor).

Lower flange tension for reinforcement

220
200
180
160
140
120
100
80
60
40
20
0
-20
-40
-60

0 20 40 60 80 100 120

Perm. Load (incl. Shrinkage and creep)
Traffic (including brake load)
Wind F * w
Temperature

²]
m
/ m
panning [N

S -80
-100
-120
-140
-160
-180

Distance from support point C [m]

Figure 64 Stresses in the lower flange of the main beams for reinforcement due to N + M y (per load group)

Tension (original) bottom flange after reinforcement

Perm. Load (incl. Shrinkage and creep)
Traffic (including brake load)
Wind F * w
Temperature

220
200
180
160
140
120
100
80
60
40
²]
m 20
/ m 0
-20 0 20 40 60 80 100 120
-40
-60
panning [N
S -80
-100
-120
-140
-160
-180

Distance from support point C [m]

Figure 65 Tensions in the original lower flange of the main beams with reinforcement due to N + M y (per load group)

It can be seen that the stresses due to the permanent loads are almost the same between the non-fortified situation and the fortified situation. This can be explained by the permanent tax alone absorbed by the unreinforced cross-section. Only the own weight of the T-piece is passed the reinforced cross-section.

It can also be seen that the stresses due to traffic loads have decreased due to the reinforced ones cross section, as expected. The tensions due to wind have remained virtually the same, because the cross-section properties have increased, but on the other hand the wind load has also increased slightly. The stresses due to the temperature load have just increased. This can be explained by the fact that it is included a vertical temperature component over the height of the main girder is subject to a load by prevented curvature. As the stiffness of the main beams has increased, so will the tension increase. However, the contribution of the temperature load in the UGT is only limited and becomes amply offset by the decrease in road tax.

The stresses in the flange of the tee are shown in the figure below.

T-piece bottom flange tension

Perm. Tax)
Traffic (including brake load)
Wind F * w
Temperature

100
80
60
40
²]
m 20
/ m

0 0 20 40 60 80 100 120

panning [N
-20

-40

-60

Distance from support point C [m]

Figure 66 Tensions in the new bottom flange (T-piece) of the main beams after reinforcement due to N + M y (per load group)

As can be seen, the stresses from the permanent loads are virtually zero, because this part alone is loaded by the weight of the T-piece.

It is concluded that the stresses in the reinforced part of the main beam in the UGT at the the top remains almost the same and decreases at the bottom. In the unreinforced section at the support points, the tensions in the UGT remain the same as in the situation before reinforcement.

5.1.3 Pleat of the body

The stresses in the main beam have decreased in the reinforced situation compared to the situation before strengthening. The tension applies only to the cut at the location of the intermediate support point (cut C) has remained virtually the same.

Section C

Figure 67 Location cut C (intermediate support point)

The test was performed again for this section, mainly because it is also required for the assessment of the jacking points. The calculation is shown in Appendix C1 .a The following follows Results.

Cut	Location dx [mm]	Voltage class 3 without stiffener [N / mm²]	Voltage class 3 with stiffener [N / mm²]	Voltage class 4 with stiffener [N / mm²]	UC normal-tensions due to bending and normal force	UC af-sliding	UC normal-power, shear force and bending	UC folds causes through flange
C (front) 79588		-319	294	-330	0.94	0.76	0.83	0.28
C (after adjust.)	79588	-318	-293	-329	0.94	0.77	0.85	0.28

Table 47 Overview of the unity checks for the bend check of the main beam (UGT)

For the tensions in the T-piece it applies that these are so low (maximum -82 N / mm² pressure) that also in the tee creases of the body will not occur. In addition, the longitudinal stiffeners (flanges) are relatively close together (350 mm), so that they will give relatively much support to the body.

5.1.4 Stability

Buckling of the existing bottom flange

In addition to the strength calculation, stability of the printed bottom flange (kinking out of plane) was checked.
The buckling length is determined in accordance with NEN-EN 1993-1-1 Appendix C.2.4.2 by using the printed bottom flange consider as a hinged beam between two k-beams, which are located at the intermediate crossbars are resiliently supported. It follows that 3.0 m can be used for the buckling length turn into.

The assessment was carried out in accordance with Article 6.3.1, whereby the lower flange was considered to be under pressure rod. For this equivalent rod is for the determination of the area and the moment of inertia based on the surface of the bottom flange plus 1/3 of the (effective) parts of the body under pressure.
The longitudinal stiffeners on pressure are also included for 1/3.

The calculation is shown in the Mathcad calculations where the bend test was also performed, because the effective part of the body must be included in the calculation. For this is please refer to Appendix C1. The results of the buckling test are summarized in the table below. from the calculations show that the beam is not sensitive to buckling of the bottom flange.

Cut	Location dx [mm]	UC
C (for adjust.)	79588	0.94
C (after adjust.)	79588	0.94

Table 48 Overview of unity checks for stability of the bottom flange of the main beam (UGT use)

Buckling of the new bottom flange

In addition to the existing bottom flange, the new bottom flange of the T-piece has also been tested for buckling stability. from the stress in the new tee follows that the greatest compressive stresses occur in fields 1 and 3, maximum -81 N / mm². For this, the lower flange plus half the body of the tee is considered a beam loaded on pressure. The buckling stability test was carried out in accordance with NEN-EN 1993-1-1 art. 6.3.1

It follows from the calculation that the maximum permissible buckling length is approx. 18 meters. Practically there is included every k-bandage a shot applied. The calculations are shown in Appendix C1. i.

Cut	Buckling length [m]	UC
Field 3	18	0.91

Table 49 Overview of unity check for stability of the bottom flange (T-piece) of the main beam (conversion)

After fitting the tee, the bulkheads are welded to the bottom flange and body of the T-piece and welded to the bottom flange of the main beams, see Figure 68 . To make a rigid connection with the transverse stiffener is also shot above the lower flange of the existing main beam welded. The application of the bulkhead on the inside (left in the figure below) is not possible, in related to the presence of the joint with the lower edge of the k-band on that side.

Figure 68 Detail of the partitions in the bottom flange T-piece

The partitions (lateral supports) must conform to NEN-EN 1993-1-1 art. 6.3.2.5 (2) dimensioned too are on the greatest of the following forces

$N_{st, Ed} = 0.01 \text{ x } A_f \text{ x } \sigma_{f, Ed} = 0.01 \text{ x } 35 \text{ x } 500 \text{ x } -81 \text{ N / mm}^2 = 14.1 \text{ kN}$
$N_{st, Ed} = 0.005 \text{ x } A_f \text{ x} f_y = 0.005 \text{ x } 35 \text{ x } 500 \text{ x } -355 \text{ N / mm}^2 = 31.1 \text{ kN}$

The lateral support is calculated on the basis of a horizontal force on the bottom of the bulkhead (shown in red). One will pass through the arm to the existing bottom flange moment that must be absorbed by a vertical tensile force through the weld between the cover plate and the bottom flange of the existing main beam and a compressive force at the location of the web (green displayed). The vertical force is 31.1 kN * 330 mm / 190 mm = 54.0 kN.

Assuming a thickness of the bulkhead of 15 mm and a spread under 45 ° over the thickness of the thickness plate (t = 20 mm) will take the load through 15 mm + 2 x 20 mm = 55 mm weld (a = 4 mm) must become. This results in a stress in the weld of $\sigma_1 = \tau_1 = 54.0 \text{ kN x } \sqrt{2} / (2 \text{ x } 4 \text{ mm x } 55 \text{ mm}) =$ 174 N / mm². This results in the next UC.

$[174^2 + 3\text{x } (174^2)]^{0.5} = 348 \text{ N / mm}^2 \leq 510 / (1.0 \text{ x } 1.25) = 408 \text{ N / mm}^2 \rightarrow \text{UC} = 0.85$

5.1.5 Long stiffeners

The tensions in the longitudinal stiffeners will of course also decrease or remain virtually the same. Because this were already satisfactory in the unreinforced situation, they have not been tested again.

5.2 Crossbars

The cross bars are likely to be only minimally affected by the reinforcement of the main beams. Given the large margin in UCs, this will not be a problem in advance expected.

The cross beams were tested for the same cross beams as in the verification calculation of the existing situation. The tandem system is placed on six crossbars, namely on the cross bars in the middle of fields 2 and 3, at the location of the intermediate supports and the end support (end cross member) and the first cross member directly next to the end support (for the deviating geometry of the end cross member.

Figure 69 Tested crossbars (shown in pink)

The final crossbars were tested in the recalculation in four sections, namely in the cantilever, just next to the cover plate in the top flange (A) and at the connection to the main beam, and in the cross beam, at the connection to the main beam (C) and in the field (D). The tensions have been compared for these 4 locations between the situation before and after reinforcement.

a BC D

Figure 70 Tested cuts of end crossbars

The other cross beams have been tested in three sections, namely at the location of the connection with the main beam (E), in the cross section with variable height (F) and in the field (G). Here too are the tensions compared between the situation before and after reinforcement.

G

EF

Figure 71 Tested cuts of crossbars

5.2.1 Stresses end cross member

The (Von Mises) stresses in the end cross member are given in the figure below, where Figure 72 shows the voltages before amplification and Figure 73 shows the voltages after amplification. In both cases assumes usage level. The figure shows the envelope of the Von Mises tensions in the entire beam (top and bottom flange). The maximum voltage occurs in the center of the field.

D

C

a B

Figure 72 Von Misses voltages in the end cross member for reinforcement (use)

Figure 73 Von Misses stresses in the end cross member after reinforcement (use)

It can be seen that the tensions in the field center have decreased somewhat, the tensions at the support point (main beam) remained the same. However, the differences are minimal, as expected.

5.2.2 Testing the final cross member

The testing of the steel in the steel-concrete beam was carried out by reading the forces in the eccentric beam element. Through the cooperation with the concrete deck there will be eccentric beam element a tensile (field) or compressive force (support point) arise in combination with the moment. This one forces and moments in the sample were then tested using Excel. This review is given in Appendix C2.

The recalculation showed that cut C was decisive for the end cross member. This cut is therefore tested again at usage level. The test results of the final crossbeam are shown in Table 50 displayed. For each column a normative force or moment is given (in bold) with the associated cutting forces from the same load combination.

Section C

	N_{min}	N_{max}	$V_{y; max}$	$V_{z; max}$	$M_{y; min}$	$M_{y; max}$	$M_{z; max}$
Normal force [kN]	**-757**	**0**	-423	-563	-749	-47	-423

Transverse force weak axis [kN]	75	0	**149**	90	72	77	149
Shear force strong axis [kN]	165	0	139	**215**	162	62	139
Moment about the strong axis [kNm]	-91	0	-13	-68	**-95**	**52**	-13
Moment about the weak axis [kNm]	22	0	56	33	22	32	**56**
UC (strength)	**0.39**	**0.00**	**0.37**	**0.37**	**0.39**	**0.23**	**0.37**
UC (stability)	**0.46**	**0.00**	**0.42**	**0.43**	**0.46**	**0.26**	**0.42**

Table 50 Overview of the unity checks for testing the final cross member (use)

The maximum UC of the final crossbeam has increased by 0.05 to UC = 0.46 due to the gain, but still amply satisfactory.

5.2.3 Tensions cross beams

Three cuts have been tested in the normal cross beams, as previously explained in 5 different sections crossbars. In Figure 74 , the maximum Von Misses are stresses for these different cuts for the amplification situation, at usage level . Figure 75 shows the same Von Mises tensions for the situation after reinforcement. The stresses in the other cross beams are shown in Appendix C2 . The stresses remain everywhere under the yield stress (f_y = 215 N / mm²).

E

G

F

Figure 74 Von Misses stresses in the normal crossbars for reinforcement (use)

E

G

F

Figure 75 Von Misses stresses in the normal crossbars after amplification (use)

It can be seen that the tensions have increased slightly at the end, while the tensions in the field are slightly decreased. This can be explained by the fact that the main beam will react slightly stiffer, and the cross beam will move therefore it will behave more like a two-sided clamped beam.

5.2.4 Testing cross bars

The cross-section tests (strength and stability) are in a similar way as for the end cross member executed. The recalculation showed that section E was normative. This is again the cut here where tensions have also increased. The test results are shown in Table 51. Observed that section E is tested as class 1 profile. The other cuts have been tested as class 3 (conservative).

Section E							
	N_{min}	N_{max}	$V_{y; max}$	$V_{z; max}$	$M_{y; min}$	$M_{y; max}$	$M_{z; max}$
Normal force [kN]	-910	5	-160	-845	-883	-90	-379
Transverse force weak axis [kN]	3	5	70	6	5	2	35
Shear force strong axis [kN]	216	70	46	238	199	74	107
Moment about the strong axis [kNm]	-25	-18	-4	-11	-25	22	-5
Moment about the weak axis [kNm]	1	0	0	0	1	0	8
UC (strength)	**0.64**	**0.18**	**0.20**	**0.58**	**0.48**	**0.20**	**0.30**
UC (stability)	**0.87**	**0.00**	**0.14**	**0.69**	**0.86**	**0.27**	**0.39**

Table 51 Overview of the unity checks for testing the normal crossbeam in section E (use)

It is concluded that the steel in the crossbars satisfies strength and stability.

5.3 K-dressings

For the assessment of the K-relationships, the envelopes of the normal stresses in the various rods determined with the help of Scia Engineer to determine the normative cross sections. The bars with the highest voltages have been tested using Excel.

5.3.1 Assessment of the lower edge of the K-bandages

Two types of bottom edge profiles have been used. The bottom edges at the supports are half DIN 30 profiles while for the lower edges of the K-bandages at the intermediate crossbars half DIE 26 profiles have been used. The enveloping tensile and compressive stresses in the UGT (usage level) in the lower edge of the K-bandages and portals are shown in Figure 76 for the situation before reinforcement and in Figure 77 for the situation after reinforcement.

Standards bottom edge at impositions

Standards bottom edge at intermediate crossbars

Figure 76 Compressive and tensile stresses in the lower edges of the K-bandages for reinforcement (use)

Standards bottom edge at impositions

Standards bottom edge at intermediate crossbars

Figure 77 Compressive and tensile stresses in the lower edges of the K-bandages after reinforcement (use)

It can be seen that the tensions at the supports increase slightly. The UC of the lower edges of the intermediate crossbars were so low in the verification calculation of the situation without reinforcement (UC = 0.22) that they have not been retested. For the lower edge of the K-bandages at the This assessment has been repeated again between support centers. The results of this review are shown in Table 52.

Lower edge for intermediate supports	N_{min}	N_{max}	$V_{y; max}$	$V_{z; max}$	$M_{y; min}$	$M_{y; max}$	$M_{z; max}$
Normal force [kN]	**-229**	**355**	355	-186	-155	-186	201
Transverse force weak axis [kN]	0	0	**0**	0	0	0	0
Shear force strong axis [kN]	6	0	0	**10**	10	8	9
Moment about the strong axis [kNm]	7	2	2	-16	**-16**	**10**	-13
Moment about the weak axis [kNm]	0	0	0	0	0	0	**0**
UC (strength)	**0.36**	**0.28**	**0.28**	**0.50**	**0.50**	**0.32**	**0.42**
UC (stability)	**0.47**	**0.00**	**0.00**	**0.75**	**0.71**	**0.55**	**0.68**

Table 52 Overview of the unity checks for the assessment of the bottom edge of the intermediate support (use)

The strength UC increases from 0.49 in the pre-reinforcement situation to 0.50 in the post-reinforcement situation, based on the level of use. For the stability test, the increase is somewhat larger, from UC = 0.61 to 0.75. For the latter UC, the combination with maximum Vz is decisive, somewhat is unusual (usually the combination of maximum M or maximum N is decisive). In the normative the moment increases slightly, but the normal force almost doubles. This is because there another combination has become normative for max Vz, which includes a different normal force.

For this combination, the strength test increases from 0.48 to 0.50, this is also the picture of the increase for the other combinations. However, in the stability test is the effect of this normal force a bit more extreme, because the UC increases on buckling from 0.09 to 0.18. Moreover, here is in the combination with chicken has another combination factor over it, which makes the UC increase more than on it would be expected at first sight.

5.3.2 Assessment of the verticalities of the K-bandages

Two types of profiles have been used for the vertical of the K-bandages. The verticals at the supports are composed of 2 half INP 32 profiles on either side of the main beam body while one half INP 32 profile was used for the vertical bars in the K-beams at the intermediate cross members. The webs of the half INP 32 profiles are welded to the web of the main beam (see Figure 79). The envelope tensile and compressive stresses in the vertical of the K-braces and portals are shown in Figure 78 displayed. The high voltages at the portals are not correct, because SCIA also includes the moments in the plane of the body of the main beam are taken into account. These will in reality not occur. The vertical of the portal at the end support was not sufficient in the recalculation and must therefore be strengthened. This will be discussed further in the review.

Standards
vertically at the fixed
intermediate support

Leading vertical
when rolling
intermediate support

Standards
vertical at
crossbeam

Standards
vertically at it
end support

Figure 78 Pressure and tensile stresses in K-bandages (UGT)

Figure 79 Cross section of the verticals at the intermediate support point (left) and the intermediate cross members (right)

For portal B of the main bridge, it has been shown that the normal force in the vertical is not constant, as in the bar model is found, but runs along the length of the bar (see Appendix C3 of the verification calculation of the main bridges). For the course of the normal force becomes conservative assumes a linearly extending normal force that is equal to the bar force at the bottom and at the top is equal to the load of two wheels (300 kN) of the tandem system lane 1 times the load factor (1.25). Please refer to the Appendix for substantiation

C3 in the main bridge verification calculations. Maintaining a linear course is conservative.

Intermediate supports

Initially, three cuts were tested for testing, on the bottom (a), just above the cover plate (b) and just below the bulkhead (c). In the cross-section test in Excel of the verticals, the contribution of the body of the main girders included in the cross-section. There is an assistant here width on both sides of the profile of 15ε * t_w . This takes into account the thickness plates on the body at the location of the intermediate supports, so that t_w = 3 * 12 mm. Allows 15 * 3 * 12 * √ (235/350) = 442 mm on either side of the body of the INP profile. taken away.

(c)

(b)

(a)

Figure 80 Tested cuts

The capacity is based on the plastic capacity of the cross-section. In section a is account kept with the extra thickness plates on the body. The body assumes f_y = 350 N / mm², for the INP profiles of f_y = 215 N / mm².

The test results of the vertical lines at the intermediate supports are shown in Tables 53 to Table 54.

Vertical of K-bandage at the fixed intermediate support point

Cut	(a)		(b)		(c)	
	N_{max}	M_{max}	N_{max}	M_{max}	N_{max}	M_{max}
Occurring normal force [kN]	**-5058**	-4760	**-3521**	-2669	**-1959**	-1615
Capacity normal force N_{pl} [kN]	**-12864**	-12864	**-5434**	-5434	**-5434**	-5434
Moment about the strong axis [kNm]	31	**-61**	69	**82**	108	**135**
Moment capacity M_{pl} [kNm]	-307	**307**	-218	**-218**	-218	**-218**
UC (strength)	**0.56**	**0.71**	**0.96**	**0.87**	**0.86**	**0.92**
UC (stability)	**0.49**	**0.53**	**0.83**	**0.71**	**0.64**	**0.65**

Table 53 Overview of the unity checks for testing the vertical of the K-band at the fixed intermediate support point (use)

Vertical of K-bandage at the rolling intermediate support point						
Cut	(a)		(b)		(c)	
	N_{max}	M_{max}	N_{max}	M_{max}	N_{max}	M_{max}
Occurring normal force [kN]	**-5139**	-4897	**-3576**	-3055	**-1987**	-1667
Capacity normal force N_{pl} [kN]	**-12864**	-12864	**-5434**	-5434	**-5434**	-5434
Moment about the strong axis [kNm]	142	**160**	16	**23**	-116	**-143**
Moment capacity M_{pl} [kNm]	-307	**-307**	-218	**-218**	218	**218**
UC (strength)	**0.86**	**0.90**	**0.73**	**0.67**	**0.90**	**0.96**
UC (stability)	**0.63**	**0.64**	**0.69**	**0.60**	**0.56**	**0.66**

Table 54 Overview of the unity checks for testing the vertical of the K-band at the rolling intermediate support point (use)

Vertical portal end supports

The testing of the verticals of the portals at the end supports showed that the verticals are on the underside (cut a) did not meet the strength requirement.

Figure 81 Tested vertical cuts

For the end support, a reinforcement has therefore been designed above the support, see Figure 82 . This one consists of a plate of 300 mm x 400 mm x 12 mm and a plate of 794 mm x 400 mm x 12 mm, both on either side of the main spar body. The reinforcement is designed in such a way that the plates continue beyond the auger points, which must also be reinforced (see section 5.6.2). The plates are welded to the web and lower flange of the main beam after removal of the jacking points, see also report T & P-BF7387-R011 for a full description of the modification. The review is again carried out, based on the level of renovation. Conservative cuts b and c are also at the renovation level tested.

Figure 82 Reinforcement measure vertical at the end support point

The cooperating width has been kept the same as in the recalculation, assuming $t_w = 12$ mm, and thus a cooperating width of 15 * 12 * √ (235/350) = 147 mm (per side). The test results of the vertical at the end support after reinforcement are shown in Table 55.

Vertical of K-bandage at the end support						
Cut	(a)		(b)		(c)	
	N_{max}	M_{max}	N_{max}	M_{max}	N_{max}	M_{max}
Occurring normal force [kN]	**-2454**	-1661	**-2059**	**-1416**	**-1085**	-830
Capacity normal force N_{pl} [kN]	**-5430**	-5430	**-2956**	**-2956**	**-2956**	**-2956**
Moment about the strong axis [kNm]	90	**121**	36	51	-88	**-115**
Moment capacity M_{pl} [kNm]	240	**240**	210	210	210	210
UC (strength)	**0.83**	**0.81**	**0.87**	**0.72**	**0.78**	**0.83**
UC (stability)	**0.61**	**0.51**	**0.76**	**0.57**	**0.52**	**0.55**

Table 55 Overview of the unity checks for testing the verticality of the K-bandages at the end supports (renovation)

Other verticals

For the testing of the verticals for the intermediate crossbars, conservatively, only the cross section of the INP profile, so without cooperating width of the body. The following follow Results.

Vertical of K-bandage on the intermediate crossbeam		
	N_{max}	M_{max}
Occurring normal force [kN]	**1.8**	1.7
Capacity normal force N_{pl} [kN]	**835**	835
Moment about the strong axis [kNm]	-10.0	**-10.9**
Moment capacity M_{pl} [kNm]	-16	**-16**
UC (strength)	**0.61**	**0.67**
UC (stability)	**0.00**	**0.00**

Table 56 Overview of the unity checks for testing the verticalities of the K-joints at the intermediate crossbeam (use)

5.3.3 Testing diagonals of K-connections

The diagonals of the K-connections and the portals consist of 2 L80x80x10 profiles. In Figure 83 , the envelope tensile and compressive stresses of the Scia bar section shown for the situation before strengthening. Figure 84 shows the tensions for the post-amplification situation.

Leading diagonal

Figure 83 Compressive tensile stresses in the diagonals of the K-bandages for reinforcement (use)

Leading diagonal

Figure 84 Compressive tensile stresses in the diagonals of the K-bandages after reinforcement (use)

The results of the assessment are shown in Table 57 .

Diagonals of the K-relations	N_{min}	N_{max}	$V_{y; max}$	$V_{z; max}$	$M_{y; min}$	$M_{y; max}$	$M_{z; max}$
Normal force [kN]	**-325**	**320**	-283	-283	-286	291	291
Transverse force weak axis [kN]	1.0	0.4	**1.4**	1.4	1.4	0.7	0.7
Shear force strong axis [kN]	1.0	0.4	1.4	**1.4**	1.4	0.7	0.7
Moment about the strong axis [kNm]	-1.1	1.1	-1.7	-1.7	**-1.7**	**2.0**	2.0
Moment about the weak axis [kNm]	1.1	1.1	1.7	1.7	**1.7**	**2.0**	2.0
UC (strength)	**0.60**	**0.60**	**0.60**	**0.60**	**0.61**	**0.64**	**0.64**
UC (stability)	**0.91**	**0.00**	**0.88**	**0.88**	**0.89**	**0.00**	**0.00**

Table 57 Overview of the unity checks for testing the diagonals of the K-relationships (use)

5.4 Concrete deck

The reinforcement will have limited influence for the concrete deck. Thus, the tension in the top flange of the main beam not significantly changed by the reinforcement, because the bending stiffness is on the one hand increased, but on the other hand the center of gravity has shifted down. It is expected that this therefore also applies to the concrete deck.

The steel beams are tested in section 5. 1 (main beam) and section 5.2 (crossbeams). The key of the concrete deck is worked out in this chapter. The following calculations have been made for this:

- Testing composite beams
- Concrete deck test in the field

For model output and calculations, see Appendix C4. b to e.

5.4.1 Testing composite beams

The steel concrete main beams and cross beams have been tested in the benchmark positions as steel concrete section. The following assessments have been carried out:

- Main spar reinforced part: maximum field moment at the center of field 3
- Main beam reinforced part: maximum point of support at the location of the transition from the prestressed section to the reinforced section in field 2
- Main beam prestressed part: maximum support moment above support point E
- Cross beam: maximum field moment at the cross beam in the center of field 2
- Cross beam: maximum point of support at the point of support point E

The tests were carried out in accordance with NEN-EN 1994-2, based on the elastic resistance capacity. To take into account the construction phasing and the varying concrete stiffness, the stresses in the steel profile, reinforcing steel reinforcement, prestressing and the concrete for each construction phase determined separately.

In H5 .4.3 it has been shown that the concrete deck remains un cracked in the characteristic combination. However in the fundamental combination will be the deck at the point of a fulcrum moment in the main beam rip. Therefore, in the assessment of the point of support of the main beam, the prestressed part the tear moment determined. The stiffness proportion of the concrete is in the determination of the cross section balance only taken up to the moment of tearing. For the cut test, the stiffness is of concrete maintained at 0 N / mm² under tension.

NB. This approach is not entirely correct for the fulcrum moment, because after tearing there again a new balance will arise. In addition, a calculation has been made based on a stiffness of concrete of f_{cd} / 1.75 ‰ = 12190 N / mm² for all phases (instead of the n method) and the moments according to the reduced tax combination. It follows that the concrete deck is above the intermediate support point just on draft (σ_c = 0.4 N / mm²) but well below the design value of the tensile strength (f_{ctd} = 1.4 N / mm²). In consultation with RWS, it was decided not to determine the exact balance in a torn condition. This will only very slightly affect the stresses in the main beam.

Project related

5.4.1.1 Effective width of composite beam

The effective width is maintained the same as in the recalculation of the situation for reinforcement. For the main beam and the cross beam, a constant effective width of 4.72 m and 1.25 m, respectively.

5.4.1.2 Testing composite cross section

The longitudinal and transverse composite beams have been tested for the envelope values of the normal force and moment. For the prestressed part, the normal pulling force (N_{Ed}) is from the model combined with the normal compressive force ($N_{Ed, vsp}$) from the separate model with which the preload is modeled.

The occurring tensions and the unity checks are shown in the table below for both the situation before reinforcement as the situation after reinforcement. For the calculations of the situation before reinforcement, please refer to the verification calculation. The calculation of the situation after reinforcement are given in Appendix C4. g.

Part	Moment	Reinforced	Voltage σ_{Ed} [MPa]				UC
			concrete	wap	Vsp.	steel	
Main beam preloaded	Fulcrum	in front of	-	54	651 [1]	-320	0.91
		after	-	67	664 [1]	-320	0.93
Main beam not prestressed Wap 2 x 45 Ø16	Fulcrum	in front of	-	50	-	235 [1]	0.67
		after	-	38	-	233 [1]	0.67
Main beam not prestressed Wap 39 + 69Ø16	Fulcrum	in front of	-	51	-	236 [1]	0.68
		after	-	40	-	236 [1]	0.67
Main spar not prestressed Field		in front of	-8.8	-73	-	339 [1]	0.97
		after	-7.6	-67	-	247 [1]	0.70
Cross beam	Fulcrum	in front of	-	59	-	-72 [1]	0.33
		after		77	-	-87 [1]	0.40
Cross beam	Field	in front of	-6.7	-33	-	129 [1]	0.60
		after	-6.6	-32	-	124 [1]	0.58

[1] *normative*

Table 58 Overview of unity checks composite beam

It can be seen that tensions in the reinforced field of the main beam decrease. At the support center there is hardly any difference. The stresses at the support point of the cross beam increase precisely because the stiffened main beam ensures a slightly larger clamping. In the field, the tension decreases again.

5.4.1.3 Checking the sliding connection

The sliding connection has not been tested again. For the main beam, the shear force will hardly be affected by the reinforcement. The influence is somewhat greater for the crossbeam, but given the UC in the situation for reinforcement (max 0.48), the sliding connection will never become normative.

5.4.2 Concrete deck assessment

5.4.2.1 Testing torque + normal force

The concrete deck does not work at the field, between the cross bars and at the location of the overhang together as a composite section. These concrete sections have therefore been tested separately for bending and normal force. The cutting forces in the deck consist of local and global effects. To the normative
To obtain global effects, the concrete sections were tested at 4 positions on the bridge.

Figure 85 Overview of test locations

To obtain the decisive local effects, 5 different cuts were tested for each location:

- Cut A: Maximum longitudinal support point (mx +) above the cross beam. The cut has a length of 2d = 300mm.
- Cut B: Maximum longitudinal field moment (mx-) between two crossbars. The cut has a length of 2d = 300mm.
- Section C: Maximum transverse field moment (my-) between two crossbars. The cut has a length of 2d = 300mm.
- Cut D: Maximum point of support (my +) in transverse direction at the cantilever (h = 300mm) The cut is taken directly next to the top flange of the main beam. The cut has a length of 2d = 500mm.
- Cut E: Maximum point of support (my +) in transverse direction at the cantilever (h = 200mm) The cut was made at the beginning of the deck bulge. The cut has a length of 2d = 500mm.

Figure 86 Overview of cuts per location

The table below shows the forces and unity checks of the normative cuts. In front of the calculations of the situation for amplification are referred to the verification calculation. The calculations of the situation after reinforcement are given in Appendix C4. f.

				Forecast.	For reinforcement			After reinforcement		
Position	Part	Cut	h	$N_{d, vsp}$	N_{Ed}	M_{Ed}	UC	N_{Ed}	M_{Ed}	UC
				[kN / m]	[kN / m]	[kNm / m]		[kN / m]	[kNm / m]	
	M_{stp} longitudinal direction	Cut 2A	200	-1372	1151	42.6	0.74	1188	42.8	0.77
	M_{field} longitudinal direction	Cut 2B	200	-1372	1055	57.8	0.68	1079	52.7	0.63
Policy Research Center E	M_{field} cross direction	Cut 2C	200	-	-98.6 [2]	63.0	0.99 [1]	-6.3 [2]	58.6	1.02 [1]
	M_{stp} transverse direction h = 300	Cut 2D	300	-	83.2	127.5	0.81 [1]	45.8	124.1	0.77 [1]
	M_{stp} cross direction h = 200	Section 2E	200	-	0.0	54.6	0.63 [1]	0.0	54.4	0.61 [1]

[1] based on linear combination of maximum moment

[2] The design variable for the normal compressive force (myD- + nyD) is conservatively set to 0 by SCIA. That is why we went out of the basic value (my + ny) of the normal force

Table 59 Overview unity checks prestressed part

				For reinforcement			After reinforcement		
Position	Part	Cut	h	N_{Ed}	M_{Ed}	UC	N_{Ed}	M_{Ed}	UC
				[kN / m]	[kNm / m]		[kN / m]	[kNm / m]	
	M_{stp} longitudinal direction	Cut 1A	200	120.5	14.4	0.36	200.9	22.1	0.63
	M_{field} longitudinal direction	Cut 1B	200	-808.8 [2]	69.0	0.64 [1]	-730.6 [2]	59.1	0.57 [1]
Middle									

field 2	M_{field} cross direction	Cut 1C 200	-244.6	64.1	0.88 [1]	-175.0	58.8	0.86 [1]
	M_{stp} cross direction h = 300	Cut 1D 300	-90.6	84.7	0.48 [1]	-86.3	87.0	0.49 [1]
	M_{stp} cross direction h = 200	Section 1E 200	-51.5	40.7	0.60 [1]	-49.2	42.0	0.62 [1]
	M_{stp} longitudinal direction	Cut 3A 200	104.6	14.7	0.36	93.0	22.0	0.53
	M_{field} longitudinal direction	Cut 3B 200	-1099.5 [2]	68.9	0.58 [1]	-930.2 [2]	49.5	0.44 [1]
Middle field 3	M_{field} cross direction	Cut 3C 200	-245.5	63.1	0.86 [1]	-181.8	58.7	0.85 [1]
	M_{stp} transverse direction h = 300	Cut 3D 300	-97.6	84.7	0.86 [1]	-87.6	86.9	0.64 [1]
	M_{stp} cross direction h = 200	Section 3E 200	-55.4	40.8	0.45 [1]	-50.7	42.1	0.47 [1]
	M_{stp} longitudinal direction	Cut 4A 200	85.3	20.2	0.48	75.9	24.6	0.58
	M_{field} longitudinal direction	Cut 4B 200	46.2	63.4	0.97	41.5	52.4	0.80
Fulcrum F	M_{field} cross direction	Cut 4C 200	-239.0 [2]	63.73	0.88 [1]	-188.5 [2]	54.3	0.78 [1]
	M_{stp} cross direction h = 300	Section 4D 300	50.1	127.7	0.79 [1]	58.5	98.1	0.61 [1]
	M_{stp} cross direction h = 200	Section 4E 200	45.0	57.5	0.69 [1]	-66.8	43.3	0.48 [1]

[1] based on linear combination of maximum moment
[2] The design variable for the normal compressive force (nyD + nxD) is conservatively set to 0 by SCIA. That is why it has been assumed the base value (ny + nx) of the normal force

Table 60 Overview unity checks armed part

In particular, the Unity Checks of cuts A (longitudinal direction, support point) in the reinforced deck are increasing. This is mainly due to the increase in temperature effects, due to the higher stiffness of the main beam by adding the tee. This is in line with the higher tension in the samples top flange of the main beam due to the temperature load. This applies to the main beam itself of the larger temperature effects on the total UC is relatively limited, because the voltages in particular determined by the permanent load. However, this does not apply to the (reinforced) concrete deck, because it only collapsed in one of the last phases, so that the forces are mainly caused by the variable loads are determined. This increases the effect on the UC. Nevertheless, the concrete section even after reinforcement. The slight overshoot in cut 2C becomes as acceptable, especially since the reduced wind load and tax combinations.

5.4.2.2 Testing shear force

The assessment of the deck for shear and punch will not change due to the reinforcement. The key is therefore not re-executed for the reinforced situation.

5.4.3 Assessment of assumption of non-cracked deck

The stiffness of the concrete is based on non-cracked concrete; see principles note H 8.4.7. On Based on the model output, it has been verified whether the assumption is correct that the entire concrete deck remains under pressure. The deck is assumed to be torn as the occurring stress in the characteristic load $_{combination}$ is greater than twice f_{ctm} . For concrete K450 this amounts to a maximum voltage of 2 * 3.02 Mpa = 6.0 Mpa.

Based on the analysis below, it was concluded that the entire concrete deck is in the final situation remains uncracked, even after the reinforcement of the main beam and the portals. In the modeling, the uncracked stiffness of the concrete is therefore correctly included.

Prestressed deck

It can be seen in Figu average compressive stress as a result of pre-stress is 6.6 Mpa is. In the right figures, the maximum tensile stresses due to the others load cases, with Figure 87 showing the situation before amplification and Figure 88 showing the situation after strengthening. Where the voltage is higher than | -6.6 | + 6.0 = 12.6MPa is the case cracked concrete.

$\sigma_{x; rep}$ bias $\sigma_{x; cart}$ other tax cases

Figure 87 Normal stresses prestressed concrete deck for reinforcement (use)

$\sigma_{x; rep}$ bias $\sigma_{x; cart}$ other tax cases

Figure 88 Normal stresses prestressed concrete deck after reinforcement (use)

It can be seen that cracking will occur very locally at the location of the supports (gray area). Given the limited size of the area (approximately 1m), the assumption is that the entire prestressed deck non-cracked is maintained. In the reinforced situation, the crack has remained virtually unchanged relative to the unreinforced situation.

Armed deck

In Figure 89 and Figu stresses are on the bottom and top of the concrete deck of field 2 and field 3 are shown for the situation before amplification and after amplification respectively. To see that the occurring longitudinal stresses in the entire armed deck are below the maximum tensile stress of 2 f_{ctm} (= 6.0 MPa). Only very local, at the bottom of the deck the tension is higher between the first two crossbars. Given the limited size of the area (approx. 1m) where the tension is higher than 6.0 MPa, the assumption is that the deck will remain uncracked enforced. There are no major differences in the situation before and after reinforcement, as expected.

σ_x field 2 σ_x field 3

Figure 89 Normal stresses (longitudinal direction) reinforced concrete deck for reinforcement σ x field 2 σ x field 3

Figure 90 Normal stresses (longitudinal direction) reinforced concrete deck after reinforcement

5.5 Inspection paths

The construction of the inspection paths is not affected by the reinforcement. For the calculation of this section refers to the verification calculation [T & P-BF7387-R005]. Corroded parts can be replaced in accordance with existing.

5.6 Bearings and jacking points

5.6.1 Impositions

Design support reactions
Support reactions were compared with capacity in a similar way as in the verification calculation of the supports. In the Scia calculation, the following support reactions are found in the situation after amplification at usage level.

Figure 91 Support reactions to UGT use

Due to symmetry, the tandem system is only applied to the right half of the bridge plus above it permanent support. The reaction force of pillar C should therefore be maintained equal to pillar F.

Testing in accordance with NEN 1337-4

Pillar C / F

When this assessment is carried out in accordance with the current standard (NEN 1337-4: 2005), a characteristic resistance of the contact pressure per unit length found from:

$$' = 23 \cdot \cdot \quad = 23 \cdot 175 \cdot \frac{600^2}{210000} = 6.90 /$$

Assuming a length of 376 mm and $\gamma_m = 1$, a capacity of

$$' = \quad {}_2 \cdot 376 = 6.90 \quad \cdot 376 = 2594$$

Assuming a support reaction at the usage level in the reinforced situation (2392 kN), a UC = 0.92 found, which satisfies the imposition.

Pillar D

For the pivot bearing of pillar D, a characteristic resistance of the contact pressure is calculated according to draft version of NEN-EN 1337-6: 2018, because the current version of this standard (NEN-EN 1337-6: 2004) an erroneous capacity formula contains:

$$= 139 \cdot \frac{\left(_9 \quad\right)^3 \cdot {}_1 \; {}^2 \cdot {}^2 \quad {}^2}{{}^2 \cdot ({}_1 - {}_2)^2} = 139 * \frac{\left(\frac{450}{1.0}\right)^3 \cdot 265^2 \cdot -250^2}{210\,000^2 \cdot (265 - 250)^2} \quad 5603$$

Based on a support reaction at the usage level (5068 kN), a UC = 0.90 is found, which means the imposition is sufficient.

Pillar E

The imposition of pillar E becomes a characteristic resistance of the contact pressure per unit length found from:

$$' \quad 600^2$$

$= 23 \cdot \cdot \quad = 23 \cdot 235 \cdot \quad 210000 \quad = 9.27 /$

Assuming a length of 516 mm and $\gamma_m = 1$, a capacity of

$= \quad _2 \cdot 516 = 9.27 \quad \cdot 516 = 4781$

Assuming a support response at usage level (5146 kN), a UC of UC = 1.08 is found .

When starting from the reduced load combinations, as described in the
starting point report sections 6.4 and 6.9, a support reaction of 4892 kN is found, with a
UC = 1.02 . So the imposition is just not enough. Given the small excess, this is considered acceptable
seen.

Fulcrum	Capacity (ULS)	Performance (for amplification) Rz [kN]	UC	Occurring (after amplification) Rz [kN]	UC
Pillar CF	2594	2359 (2228)	0.91 (0.86)	2392 (2259)	0.92 (0.87)
Pillar D (fixed solution)	5603	5022 (4767)	0.90 (0.85)	5068 (4817)	0.90 (0.86)
Pillar E (roll up)	4781	5092 (4835)	1.06 (1.01)	5146 (4892)	1.07 (1.02)

Table 61 Comparison of support reactions for use level with calculated capacity in accordance with NEN-EN 1337

It is concluded that the vertical support reactions are sufficient, provided that there is no material removal
by corrosion.

Horizontal support reactions in transverse direction

No design capacities of the supports are known. Therefore, the capacity is determined analogously
to the (re) calculation [BBV0010-01]. According to SCIA, the horizontal support reactions below are
found it.

Figure 92 Horizontal support reactions UGT use

Pillar C and F

The capacity is determined analogous to the recalculation [BBV-0010-01]. It is decisive
pressure surface (cam) on the top and bottom of the roll. In the recalculation [BBV-0010-01] is erroneous
assumes a capacity of 2x tensile strength. This appears to be an error and has therefore not been applied.

Figure 93 Fragment of calculations for ridge supports 158 tons and 203 tons from [BBV-0010-01]

Based on the new taxes, the following calculation can be made analogously.

Pillar C and F

F_h = 234 kN (ULS)

$\sigma_{vl.dr}$ = 234 kN / 16.5 cm² = 142 N / mm²

$f_{vl.dr}$ = 340 N / mm²
UC = 137/340 = 0.42

$\tau_{f, Ed}$ = 234 kN / 16.5 cm x 2.8 cm = 50.6 N / mm²
$\tau_{f.Rd}$ = 0.58 * 340 N / mm² = 197 N / mm²

UC = 50.6 / 197 = 0.26

Pillar E

F_h = 460 kN (ULS)

$\sigma_{vl.dr}$ = 460 kN / 16.5 cm² = 278 N / mm²

$f_{vl.dr}$ = 340 N / mm²
UC = 278/340 = 0.82

$\tau_{f, Ed}$ = 460 kN / 16.5 cm x 2.8 cm = 100 N / mm²
$\tau_{f.Rd}$ = 0.58 * 340 N / mm² = 109 N / mm²

UC = 100/197 = 0.51

Pillar D (fixed imposition)
No horizontal capacities have been given for the supports at the location of pillar D (fixed support). Also in the recalculation no further calculation is made of the horizontal capacity of the fixed support points. Therefore, no statement can be made whether this is sufficient. Can be considered be recalculated.

	For reinforcement			After reinforcement		
Fulcrum	Ry [kN]	UC busy	UC shear	Ry [kN]	UC busy	UC shear
Pillar CF	219	0.39	0.24	234	0.42	0.26
Pillar D (fixed imposition)	283			312		
Pillar E (role of imposition)	429	0.76	0.47	460	0.82	0.51

Table 62 UC's supports before and after reinforcement (UGT use)

Longitudinal support reactions

In pillar D, in addition to the support reactions in the transverse direction, support reactions in the longitudinal direction also occur. The figure below shows the support reactions found. The same applies to the longitudinal direction horizontal capacities of the support are given in the design and recalculations. You can do this therefore no statement is made as to whether it is sufficient. It is recommended to recalculate this to feed. It is noted, however, that the horizontal support reactions in the longitudinal direction are relatively high and in are largely caused by the fully fixed modeled supports. In fact the bearings have play, so that the coercive forces will be lower. Relative to situation for reinforcement (728 kN), the horizontal forces have decreased somewhat, which can be explained because the wind load is slightly lower, because the reduced wind load has been taken into account. This reduction is greater than the increase due to the higher main girders.

Figure 94 Horizontal support reactions in the longitudinal direction UGT use

Responses per tax case

To gain more insight into the tax payments of the various tax cases, see the table below shows the contributions of the various tax components (without tax factor) summarized.

		Pillar CF			Pillar D (fixed solution)			Pillar E (roll up)		
		$R_{X, max}$	$R_{Y, max}$	$R_{Z, max}$	$R_{X, max}$	$R_{Y, max}$	$R_{Z, max}$	$R_{X, max}$	$R_{Y, max}$	$R_{Z, max}$
ULS (usage) [kN]		0	234	2392	709	312	5068	0	460	5146
BGT (cart)	[kN]	0	178	1950	528	216	4173	0	336	4234
Permanent	[kN]	0	32	846	0	5	2223	0	60	2248
Traffic	[kN]	0	48	955	17	24	1609	0	29	1620
Brakes	[kN]	0	5	13	325	1	3	0	1	12
Wind F * w	[kN]	0	92	137	194	170	320	0	216	337
Temperature	[kN]	0	68	67	1	57	67	0	74	72

Table 63 Results of load cases for reaction forces

The permanent load and the traffic load make the greatest contribution to the support forces. It
effect of temperature and brake loads is small compared to the contribution of wind load.

5.6.2 Auger points

Jacking points at the location of the intermediate supports
The jacking points are tested against the bearing stress at the location of the body, in the cut just above the bottom flange. This bearing pressure has increased slightly due to the new T-piece. In addition, there is an assessment carried out of the transverse load in the body of the main beam, which should be tested for the interaction with longitudinal tensions (fold). The calculation is included in the pleat assessment of the main beam of section C, see Appendix C1 .

Imposition tension body and stiffener
In the cut in the body just above the bottom flange, a test is performed on the comparison voltage, outgoing of a spread of the support pressure at 45 ° in the bottom flange. There are stiffeners on both sides of the body which are included in the surface. The bridge is assumed to be fully loaded during jacking and each jacking point absorbs 50% of the load (hydraulically coupled augers).

Figure 95 Mounting surfaces of jacking points at pillar B

The results are summarized in the table below. For the body, the longitudinal stresses.

Fulcrum	For reinforcement			After reinforcement		
	$\sigma_{cf., Ed}$ [N / mm 2]	f_{yd} [N / mm 2]	UC	$\sigma_{cf., Ed}$ [N / mm 2]	f_{yd} [N / mm 2]	UC
Pillar E (body)	329	350	0.94	329	350	0.94
Pillar E (stiffener)	138	215	0.40	140	215	0.40

Table 64. Overview unity checks bearing pressure above jacking points (UGT use)

The increase in stresses due to the gain is minimal and can be explained by the increase of the own weight by the tee.

Cross-sectional load assessment
It is assumed that the transverse load above the jacking points is partly through the thickening plates transferred to the transverse stiffener above the normal support point. The other part is through the web plate paid yourself. For the distribution of taxes between these two systems it is assumed that these are divided on the basis of the thickness of the different plates. The tensile strengths are tested pressure diagonals in the thickening plates and the interaction between fold and transverse loads in the body above the jacking points, see Appendix C1.b and c.

Figure 96 Payment of the transverse loads in the thickening plates at pillar E

In the interaction formula, the combination of the bending moment and transverse load is tested. The maximum transverse load occurs with traffic above the support, while the maximum moment occurs in traffic in the field. Therefore, the interaction formula is assumed to be at the maximum when 80% of the transverse load is present.

Fulcrum	For reinforcement			After reinforcement		
	$\sigma_{cf., Ed}$ [N / mm 2]	f_{yd} [N / mm 2]	UC	$\sigma_{cf., Ed}$ [N / mm 2]	f_{yd} [N / mm 2]	UC
Pillar E (printing diagonal)	263	350	0.75	266	350	0.76
Pillar E (drawstring)	155	350	0.44	157	350	0.45
Pillar E (transverse load η_2)	$UC = \eta_2 = F_{vp} / F_{Rd}$		0.73	$UC = \eta_2 = F_{vp} / F_{Rd}$		0.74
Pillar E (pleat interaction and transverse	$UC = (0.8 * \eta_1 + 0.8 * \eta_2) / 1.4$		0.96	$UC = (0.8 * \eta_1 + 0.8 * \eta_2) / 1.4$		0.96

Table 65 Overview unity checks bearing pressure above jacking points (UGT use)

The increase in stresses from the gain is minimal.

Jacking points at the end supports

In the current situation, the jacking points at the end support points are not able to traffic load, because on the one hand the support block under the lower flange is too narrow (200 mm) to to be able to introduce the bearing forces (in particular the moment in the plane of the portal) into the flanges of the

½ INP32 profiles on both sides of the body. In addition, the ½ INP32 profiles are above the auger point only 300 mm long, so that the tension will have to be fully absorbed in the body, which will result in pleat of the body. This will never suffice under full traffic load, especially given the UC from the normal end support point, which does have a full transverse stiffener above the support.

Figure 97 Side view of the current jacking points at the end supports

Figure 98 Bottom view of the current jacking points at the end supports

As a reinforcement measure, the same bearing surface must be created on the bottom as with the end bearings for the introduction of force in the jacking point and the ½ INP profiles above the auger points to be longer, in order to transfer the force over sufficient length to the end portal / to be able to enter from the body of the main beam. The existing ½ INP32 is used for this profiles above the auger point and the auger plate below the bottom flange (200x200x38 mm) (shown in red). The thickening plates that are added for the reinforcement of the verticals above the end supports must continue beyond the jacking points. Then submit on the other side of the body / the screed plates 1/2 INP32 profiles to be applied above the auger point the outside extends almost to the top and on the inside just below the longitudinal stiffener continues. A new screw plate of 300x300x38 mm should be used under the bottom flange.

Figure 99 Reinforcement of jacking points at the end supports

Over the length of the transverse stiffener above the jacking point, the forces will gradually become through the body transferred to the transverse stiffener above the end support and to the main beam web (introduction shear force). The dimensions of the profiles are based on the same cross sections as the transverse stiffeners at the end support. The strength test therefore corresponds to that of the verticals of the k-bandages at the end bearing, see section 5.3.2 . The support block is below the bottom flange chosen so that the force can be fully guided into the flanges of the ½ INP32 profiles and the cooperating width of the body (147 mm on either side of the stiffeners).

6 Assessment of connections

The following connections were tested for strength in the verification calculation.

- Type 1 - welding connection bottom flange main beam
- Type 2 - rivet connection section division main beam
- Type 4 - horizontal connection K-connection with cross stiffener
- Type 7 - connection crossbars with main beam
- Type 9 - connection diagonals

For each connection it was examined whether there is an increase in the forces or the stresses in the link. If this is the case, the connection has been tested again for strength. In addition, the following new connections checked.

- Type 25 - Welded connection at the end of the tee
- Type 26 - Casing V-seams

6.1 Connection: Type 1

The top plate is welded to the bottom flange of the main beam with a fillet weld. The welded joint must have the transfer tension in the thickener plate to the bottom flange of the main beam. In the verification calculation is demonstrated that the welded connection is adequate in the current situation. In the amplified situation, the voltage is in the cover plate because the T-piece under the bottom flange extends beyond the ends of the sheet plates are extended. In addition, the existing weld has been expanded from a weld a = 4 mm to a = 8.6 mm.

Figure 100 Reinforcement of the welds on the ends of the thickening plates.

Because both the force to be transmitted has decreased, and the throat diameter has increased, the connection will also in the reinforced situation.

6.2 Connection: Type 2

The sections of the main beam are located at the beginning and end of the prestressed section concrete deck. At the section division, both parts of the main beam are marked with a rivet connection interconnected.

Figure 101 Side view of connection type 2

The calculations in the current situation without amplification have shown that the connection is sufficient. The reinforcement with the T-piece is also used in the section with the section division. The tensions will decrease as a result, as shown in the strength calculation. The connection will therefore also be in meet the reinforced situation.

6.3 Connection: Type 4

The bottom edge of the k-ties are with the bottom flange of the main beam and the cross stiffener connected. This connection is not the same for all K-bandages, so there is a difference in the profile type and the rivet distances between the joint in the lower edge of the portal at the supports and the intermediate k-relationships. In the verification calculation, a distinction is made between type 4-1 (intermediate k-bandages) and 4-2 (k-bandage on the support).

For the intermediate k-relationships, a maximum UC in the compound of 0.20 was found in the current situation. In the fortified situation there will be no significant change of forces performance. Therefore, this connection has not been tested again.

At the location of the intermediate supports, the horizontal bottom edge consists of a ½ DIN 30 profile.

Figure 102 Connection horizontals of K-connections with the main beams with fixed support.

The rivets, welded joint and net cross-section were tested again using Mathcad, see Appendix D1. The connection at the location of the permanent support is decisive. The results of the calculations are summarized in Table 66 .

Detail Type 4-2: Connection between lower edge of K-bandages and main beam (fixed intermediate support)

Test aspect	Bottom flange	Body	Connecting plate	Kneepad
Shear rivets	1.00 (0.97)	1.15 (1.15)		
Net cross-section	0.26 (0.26)	0.75 (0.73)	0.55 (0.55)	0.75 (0.73)
Weld connection				0.22 (0.21)

Table 66 Test results of the connection between horizontal and main beam in the fixed support (use).

It can be seen that shearing of the rivets in the body is no longer sufficient. For comparison, in the present situation before reinforcement was UC = 1.00. Also under the reduced load combinations is sufficient this connection, see Appendix D1c . Shearing of the rivet is decisive, but the butt is sufficient. The 3 rivets (around 20) in the body should therefore be replaced.

A fitting bolt M20, quality 8.8 was chosen, because the friction with a pretension injection bolt is not can be guaranteed by the coating between the two plates and the resin has insufficient strength to prevent the bolt from moving. If during drilling it appears that the hole does not meet the

requirements regarding the hole tolerances for an M20, the hole must be drilled into an M24 fitting bolt.
For a full description of the steps to be taken, please refer to report T & P-BF7387-R011.

Figure 103 Reinforcement of lower edge at the location of fixed support

The calculation of the bolt connection is shown in Appendix D1d and has been carried out at the renovation level.
This finds a UC of 0.67 for the bolt connection in the body.

Detail Type 4-2: Connection between lower edge of K-bandages and main beam (fixed intermediate support) (body with adjusting bolts)

Test aspect	Body	Kneepad
Shear rivets	0.79	
Net cross-section	0.78	0.78
Weld connection		0.23

Table 67 Test results of the connection between horizontal with main beam at the fixed support (connection body with adjusting bolts).

Because the connection at the fixed intermediate support point is not sufficient, the connection is also at the rolling intermediate support point checked. This appears to be satisfactory. This can be explained by the fact that there are more here load via the vertical is supported by the rotational clamping, and therefore less via the diagonals and bottom edge.

Detail Type 4-2: Connection between lower edge of K-bandages and main beam (rolling intermediate support)

Test aspect	Bottom flange	Body	Connecting plate	Kneepad
Shear rivets	0.84	0.84		
Net cross-section	0.21	0.36	0.44	0.36
Weld connection				0.17

Table 68 Assessment of the results of the connection between horizontal and main beam in the fixed support.

It is concluded that the connections between the lower edge of the K-braces and the main beam in the fortified situation.

6.4 Connection: Type 7 and 10, 11 and 12

For testing the connections of the crossbars to the main beam, console and the diagonal of the K-bandages, a distinction has been made between the end cross members (type 7) and the others cross bars (type 10, 11 and 12).

6.4.1 End crossbars: Type 7

The end crossbars are connected to the body of the main beam with a head plate with rivets. The head plate is fixed with a fillet weld on both sides of the body and the flange of the cross beam. The consoles are connected to the main beam in the same way . Figure 104 shows the geometry of the connection at the end cross member.

Center of gravity
link

Draw zone

Center of gravity cross beam Neglected
in calculation

Pressure zone

Pressure zone

Figure 104 Overview of connection between end cross member and consoles

The internal forces in the crossbeam and the diagonal of the K-brackets are transmitted through this connection transferred to the main beam. Due to the stiffening of the vertical sections of the portal at the end support point the forces in the joint may have changed. The connection has therefore been re-tested for the new forces. The calculation method is the same as in the verification calculation and is below repeated.

The rivets, welded joints and the net cross sections were tested using Mathcad; see Appendix D2. Here it is assumed that in the cross section at the location of the connection the bulkhead, including flange, acts under the cross beam as a pressure point. For the calculation, the flange of the bulkhead is (150x12 mm) and a part of the body of the bulkhead (200 mm) included as pressure point (shown in red in above figure). The reinforcement of the flange of the bulkhead has been neglected for testing. It other part (bottom flange cross beam, cross beam body and top part beam bulkhead) are not included in the cross-section, because here there is a relatively weak connection (head plate that is perpendicular to its plane tension is loaded) (shown in black). Namely, the top flange on pull (shown dark blue) will react much stiffer, because the plates of the top flange continue over the main beam.

The difference in the center of gravity of the normal force of the cross beam (shown in purple in Figure 104) and the normal and transverse force of the diagonal (shown in blue in Figure 104) relative to the connection (shown in green in Figure 104) have been included in the calculation as a supplement to the moment.

The results of the calculations are summarized in Table 69. The calculation shows that all assessments. The UCs are virtually the same as in the unreinforced situation.

Detail Type 7: Connection between end cross beam and main beams

Test aspect	Rivets top flange	Rivets body	Weld in the body	Weld in the bulkhead	Net cross section
Console	0.17	0.13	0.22	0.43	0.31
End cross member	0.22	0.19	0.50	0.74	0.53

Table 69 Unity checks connections in end cross member.

6.4.2 Other crossbars: Type 10, 11 and 12

The other crossbars (DIE 45) are connected to the body with a welded head plate and rivets of the main beams. The top flange and part of the body of the cross beam are at the location of the head plate removed for shear connection in the concrete deck; see Figure 105 .

Draw zone

Center of gravity link

Center of gravity cross beam (Steel-concrete section)

Neglected in calculation

Pressure zone

Pressure zone

Figure 105 Overview of connection between cross beams and main beam.

The maximum stresses occur in the intermediate cross beam at the location of the rolling intermediate support point (type 11). The cross bars at the location of the other K-bandages (type 10) and the intermediate ones crossbars (type 12) have lower stresses.

The calculation shows that a large part of the steel cross-section at the connection remains under pressure. In front of the calculation is therefore the flange of the bulkhead (150x12 mm), the web of the bulkhead, the lower flange of the cross beam and part of the body of the cross beam (200 mm) included as pressure point (red shown in Figure 105). The upper part of the body is subjected to tensile stress and is not included the cross section (shown in black in Figure 105), because there is a relatively weak connection here (end plate that is subjected to tension at right angles to its plane). The tensile load in the top flange is included by the anchor welded to the top flange.

The cutting forces are determined in the composite composite beam, with a cooperating width of 1.25 m. The difference in the center of gravity of the steel-concrete cross-section of the cross beam (purple shown in Figure 105) and the normal and shear force of the diagonal (light blue shown in Figure 105) relative to the center of gravity of the connection (shown in green in Figure 105) the calculation included as a supplement at ns, see Appendix D2. The results are presented in

Detail Type 10, 11 and 12: Connection between cross beam and main beams

Test aspect	Rivets body	Weld into the body	Read in the bottom flange	Read in the shot	Net cross-section underside
Other cross bars	0.40	0.60	0.55	0.81	0.58

Table 70 Unity check overview of the connections between crossbeam and main beam.

6.5 Connection: Type 9

Two types of connections were tested for the diagonals in the verification calculation; the connection to the top with the cross beam (type 9-1) and the connection on the bottom with the horizontal (type 9-2). The top of the diagonals was decisive. This connection has therefore been tested again.

6.5.1 Connecting diagonals to cross bars: Type 9-1

The diagonals consist of two corner profiles L80x80x10 and are riveted gusset plate connection connected to the cross beam. The sketch plate is connected to a fillet weld the flange of the bulkhead between the cross beam and cross stiffener; see Figure 106 .

Figure 106 Connection diagonals of K-connections with the crossbars,

The rivets, the welded joint and net cross sections were tested using Mathcad. The design forces in the connection have been determined using SCIA and are given in Appendix D3 . The diagonal at the fixed supports is decisive. The results of the calculations are summarized in Table 71 .

Detail Type 9-1: Connection between diagonals and cross bars

Test aspect	Shear rivets	Net cross-section profile	Net cross-section sketch plate	Read link
Western side	0.85	0.75	0.65	0.41

Table 71 Assessment of the results of the connection between diagonals with cross beams

6.6 Connection: Type 25 - Weld connection at the end of the tee

6.6.1 Weld connection body - flange existing main beam

Between the web and the flange and between the flange and the top plate of the existing main beams is a fillet weld a = 4 mm.

Figure 107 Fillet weld between bottom flange and body and between thickening plate and bottom flange

By adding the T-piece, more shear stress will pass through this connection, especially to the end of the T-piece, because here the stresses in the T-piece have to be transferred to the existing main beam. The shear stresses due to self weight and permanent loads, before fitting the tee, are determined using the following formula.

=

For S_y , the surface of the shearing part is taken. For the reinforcement with the T-piece exists this only from the bottom flange with thickening plate. Conservatively, the maximum shear force is assumed location of the support point. The shear stress in the body is converted to the shear stress in the weld with $\tau_{weld} = \tau_{Ed} * (t_{w} / 2a)$. The shear stress in the weld due to the permanent load, inclusive load factors, is 72 N / mm², see Appendix D4.

The shear stresses due to the variable loads and T-piece weight are similar manner as in the fatigue calculations determined with a local plate model, where on the right the normal voltage as a result of the variable load plus dead weight T-piece (UGT rebuild) the model is placed.

Figure 108 Fillet weld between bottom flange and body and between thickening plate and bottom flange

The shear stress in the existing web at the end is a maximum of 40 N / mm². Translated to the weld, this is 60 N / mm². This brings the total shear stress to 132 N / mm² (UGT renovation).

6.6.2 Welded body T-piece - lower flange existing main beam

Between the body of the T-piece and the bottom flange of the existing main girders is a fillet weld a = 5 mm fitted.

Figure 109 Fillet weld between body T-piece and bottom flange

The shear stress in the body of the T-piece at the location of the welded connection to the bottom flange is maximum 100 N / mm². Translated to the weld, this is 150 N / mm² (UGT conversion), resulting in a UC = 0.74. Hereby conservatively assumes a fillet weld, in reality the end of the tee becomes complete welded over 1000 mm.

6.6.3 Welding connection body T-piece - bottom flange T-piece

A fillet weld a = 7 mm is fitted between the body of the T-piece and the bottom flange of the T-piece.

Figure 110 Fillet weld between T-piece body and T-piece bottom flange

The shear stress in the body of the T-piece at the location of the welded connection with the bottom flange of the T-piece is 140 N / mm². Translated to the weld, this is 150 N / mm² (UGT renovation), resulting in a UC = 0.73.

6.6.4 T-piece stresses

Due to the shape of the T-piece, stress concentric can also arise in the body plate itself.
It was checked whether the Von Mises stresses in the body and the flange of the tee under the yield stress remain (f_y = 355 N / mm²). The highest stresses are applied and remain well below the yield stress (UC = 0.86).

Figure 111 Von Mises stresses at the end of the tee

6.6.5 Summary of results

The results are summarized in the table below. All test aspects are sufficient.

Detail Type 25

Test aspect	τ_{las} or σ_E [N / mm²]	UC
Fillet weld body - bottom flange existing main beam	132	0.65
Fillet weld body tee - bottom flange existing main beam	150	0.74
Fillet weld body tee - bottom flange tee	150	0.73
Von mises tensions	301	0.86

Table 72 Test results for connections at the end of the tee

6.7 Connection: Type 26 - Casing V-seams bottom flange

As described in section 4.5 , for joints 5-1 and 5-2 it is necessary to insert the V-seams in the overvault existing bottom flange. For these connections, a cover has therefore been designed the function of the original welds will take over if they fail. For the two strips are used both above and below the current lower flange (160x30), which are connected by means of prestressed injection bolts (M27 10.9). The starting point is that first the v-seams are first grit, the T-piece is applied and only then the enclosure is installed.

Figure 112 Housing V-seam existing bottom flange

The calculation is based on 2x8 pretension injection bolts per side. The connection is designed to the full occurring force (UGT renovation) in the (existing) bottom flange, after reinforcement with the T-piece, to include. The enclosure is therefore able to completely transfer the tension in both flange plates can take. This is conservative, since the top flange plate should in principle not be able to enter rip. The calculation is based on the combined resistance of friction plus butt of the injection resin. The starting point is a synthetic resin of the brand Araldite SW404 with a harder HY2404, for which, in accordance with the ROBK, a (lower limit) for the design value of the compression stress of 150 N / mm² (long duration) applies.

The surfaces between the plates must be pre-blasted and coated ethyl zinc silicate so that a class B of the friction surface is obtained in accordance with NEN-EN 1993-1-8 ($\mu = 0.4$). The pretension on the bolt is maintained as 70% of f_{ub} . The connection has been calculated using Mathcad and is shown in Appendix D5. The results of the calculation are shown in the table below.

Detail Type 26

Test aspect	Shear bolts	Butt resin + friction	Net intersection profile	Net intersection sketch plate
Western side	0.85	0.78	0.83	0.92

Table 73 Test results of the enclosure

At the location of the existing transverse stiffeners (connection 5-2) the pattern will be slightly different and will the transverse stiffener must be shortened. With the application of the reinforcement in the bottom flange serves also the transverse stiffener to be reconnected to the canopy. This is based on a bolt connection with an angle steel L200x100x8, which is connected to one of the preload injection bolts in the bottom flange.

Figure 113 Casing V-seam existing bottom flange with cross stiffener

7 Conclusions

In this report, a number of reinforcements have been designed for the bridges of the IJssel Bridge tested the structural strength, stability and fatigue of the existing and new parts. The reinforcements are designed in such a way that the bridge has a residual life of (at least) 30 years. The main reinforcement is the fitting of a T-piece over almost the entire length of the main beams, with the exception of the part at the supports, in combination with the burr grinding and possibly re-applying various welds. In this way, the present becomes fatigue damage is removed and, on the other hand, the voltage fluctuations that cause the fatigue damage causes decreased.

In addition to the aforementioned reinforcement of the main beam for fatigue, there are a number of additional locally reinforcements necessary. This concerns the following reinforcements:

- Casing v-seams lower flange (fatigue) (sections 4.5 and 6.7)
- Bottom vertical portal end supports (strength) (section 5.3.2)
- Jacking points end supports (strength) (section 5.6.2)
- Connection lower edge of fixed supports (connection) (section 6.3)
- Connections knee joint cross beam - longitudinal stiffener - transverse stiffener and end support (section 4.9) **and** intermediate support point (section 4.10)

Appendix A

Input geometry SCIA Engineer

IJssel Bridge

Project related

Appendix B

Import taxes SCIA Engineer

IJssel Bridge

Appendix C

Testing for strength and stability

IJssel Bridge

Appendix C1

Main beam assessment

IJssel Bridge

Appendix C2

Assessment of crossbars

IJssel Bridge

Appendix C3

Assessment K-relationships

IJssel Bridge

Appendix C4

Concrete deck assessment

IJssel Bridge

Project related

Appendix D

Assessment of connections

IJssel Bridge

Page 127

Project related

Appendix D1

Detail type 4 - Bottom edge joint K-bandage - main beam

IJssel Bridge

Appendix D2

Detail type 7, 10, 11 and 12 - Crossbars / consoles connection - main beam

IJssel Bridge

Appendix D3

Detail type 9 - Connections diagonals

IJssel Bridge

Appendix D4

Detail type 25 - Connection end T-piece

IJssel Bridge

Appendix D5

Detail type 26 - V-seam casing

IJssel Bridge

Appendix E

Fatigue test

IJssel Bridge

Project related

Appendix E1

Detail type 1 - Weld end of the cover plate

IJssel Bridge

Appendix E2

Detail type 2 - Riveted connection in section parts of the bridge

IJssel Bridge

Project related

Appendix E3

Detail type 3 - Vertical stiffeners inside weld with the bottom flange

IJssel Bridge

Appendix E4

Detail type 4 - Riveted connection cross bracing with main beams

IJssel Bridge

Appendix E5

Detail type 5 - Welded joint in section of the bridge

IJssel Bridge

Appendix E6

Detail type 6 - Flank weld in between cover plate and bottom flange

IJssel Bridge

Appendix F

Fatigue test - na strengthening

IJssel Bridge

Project related

Annex F1

Detail type 1 - Weld end of the cover plate

IJssel Bridge

Project related

Appendix F2

Detail type 2 - Riveted connection in section parts of the bridge

IJssel Bridge

Page 142

Project related

Appendix F3

Detail type 3 - Vertical stiffeners inside weld with the bottom flange

IJssel Bridge

Appendix F4

Detail type 4 - Riveted connection cross bracing with main beams

IJssel Bridge

Appendix F5

Detail type 5 - Welded joint in section of the bridge

IJssel Bridge

Appendix F6

Detail type 6 - Flank weld in between cover plate and bottom flange

IJssel Bridge

Appendix F7

Detail type 13 - Flank weld between the main beam body and lower flange

IJssel Bridge

Project related

Appendix F8

Detail type 14 - Connection transverse stiffener - longitudinal stiffener - shot final dw. dr.

IJssel Bridge

Project related

Appendix F9

Detail type 15 - Connection transverse stiffener - longitudinal stiffener - shot in between. dr

IJssel Bridge

Project related

Appendix F10

Detail type 17 - Vertical pleat stiffener - Weld with the main beam

IJssel Bridge

Appendix F11

Detail type 20 - Weld connection location of body T-piece recess

IJssel Bridge

Appendix F12

Detail type 21 - Weld connection bulkhead bulkhead bulkheads

IJssel Bridge

Appendix F13

Detail type 22 - Longitudinal weld T-piece with flanges

IJssel Bridge

Appendix F14

Detail type 24 - Weld connection end body tee

IJssel Bridge

Project related

Appendix F15

Detail type 25 - Weld connection end body tee (shear stress)

IJssel Bridge